fractal and fractional

Article

Radial Basis Functions Approximation Method for Time-Fractional FitzHugh–Nagumo Equation

Mehboob Alam [1,*], Sirajul Haq [1], Ihteram Ali [2], M. J. Ebadi [3,*] and Soheil Salahshour [4,5,6]

[1] Faculty of Engineering Sciences, GIK Institute, Topi 23640, Pakistan; siraj@giki.edu.pk
[2] Department of Mathematics and Statistics, Women University, Swabi 23430, Pakistan; ihteramali60@gmail.com
[3] Department of Mathematics, Chabahar Maritime University, Chabahar 9971756499, Iran
[4] Faculty of Engineering and Natural Sciences, Istanbul Okan University, Istanbul 34959, Turkey
[5] Faculty of Engineering and Natural Sciences, Bahcesehir University, Istanbul 34353, Turkey
[6] Department of Computer Science and Mathematics, Lebanese American University, Beirut P.O. Box 13-5053, Lebanon; soheil.salahshour@okan.edu.tr
* Correspondence: mehboobalam.ma92@gmail.com (M.A.); ebadi@cmu.ac.ir (M.J.E.)

Abstract: In this paper, a numerical approach employing radial basis functions has been applied to solve time-fractional FitzHugh–Nagumo equation. Spatial approximation is achieved by combining radial basis functions with the collocation method, while temporal discretization is accomplished using a finite difference scheme. To evaluate the effectiveness of this method, we first conduct an eigenvalue stability analysis and then validate the results with numerical examples, varying the shape parameter c of the radial basis functions. Notably, this method offers the advantage of being mesh-free, which reduces computational overhead and eliminates the need for complex mesh generation processes. To assess the method's performance, we subject it to examples. The simulated results demonstrate a high level of agreement with exact solutions and previous research. The accuracy and efficiency of this method are evaluated using discrete error norms, including L_2, L_∞, and L_{rms}.

Keywords: fractional differential equation; meshless method; radial basis functions; FitzHugh–Nagumo equation; stability

check for updates

Citation: Alam, M.; Haq, S.; Ali, I.; Ebadi, M.J.; Salahshour, S. Radial Basis Functions Approximation Method for Time-Fractional FitzHugh–Nagumo Equation. *Fractal Fract.* **2023**, 7, 882. https://doi.org/10.3390/fractalfract7120882

Academic Editor: Rajarama Mohan Jena, Snehashish Chakraverty and Stanislaw Migorski

Received: 27 October 2023
Revised: 17 November 2023
Accepted: 6 December 2023
Published: 13 December 2023

1. Introduction

In recent years, the FitzHugh–Nagumo equation has garnered significant attention among physicists and mathematicians due to its critical role in mathematical physics. This equation finds applications in diverse fields, such as flame propagation, logistic population growth, neurophysiology, branching Brownian motion processes, autocatalytic chemical reactions, and nuclear reactor theory [1]. The FitzHugh–Nagumo equation is a nonlinear reaction–diffusion equation given by

$$u_t = u_{xx} + u(u-\beta)(1-u), \quad t > 0,\ x \in \Omega. \tag{1}$$

In the context of modeling nerve-impulse propagation [2,3], u represents the electrical potential transmission across the cell membrane. This equation elegantly combines diffusion and nonlinearity, with the behavior governed by the term $u(u-\beta)(1-u)$.

Many researchers have extensively investigated FitzHugh–Nagumo Equation (1). Notably, Shih et al. [4] explored this equation, revealing its applications in the domains of population dynamics and circuit theory. Kawahara and Tanaka [5] obtained solutions for the FitzHugh–Nagumo equation through the Hirota method. Nucci and Clarkson [6] derived solutions employing Jacobi elliptic functions. Li and Guo [7] conducted an examination and discovered a novel series of exact solutions using the first integral technique. Furthermore, Abbasbandy [8] determined soliton solutions through the homotopy analysis scheme. The FitzHugh–Nagumo equation attracted the attention of Kakiuchi and

Tchizawa [9], who obtained an explicit duck solution and delay. Schonbek [10] delved into FitzHugh–Nagumo equation in the context of boundary value problems. Yanagida [11] studied the equation's stability concerning traveling front solutions. Jackson [12] explored semidiscrete estimates for the FitzHugh–Nagumo equation. Additionally, Gao and Wang [13] discussed the existence of wavefronts and impulses in FitzHugh–Nagumo models. Employing the pseudo-spectral technique, Olmos and Shizgal [14] examined the FitzHugh–Nagumo equation. Dehghan et al. [15] investigated the FitzHugh–Nagumo equation using semianalytical techniques. The trajectory of arbitrary (real or complex) ordered derivatives exhibits nonlocal behavior when interpreted as fractional derivatives with memory indices [16,17]. This finding implies that when modeling real-world problems using fractional-order derivatives and integrals, there is a memory effect. In other words, the future state of a system not solely is determined by its current state but also takes into account its past states [18,19]. Consequently, FitzHugh–Nagumo Equation (1), which deals with arbitrary-order derivatives, can be seen as an extension of the traditional FitzHugh–Nagumo Equation (1).

Numerous authors have highlighted the practicality and significance of fractional-order derivatives and integrals in mathematical modeling within various scientific and engineering domains [20–23]. Given the ongoing research in this field and its importance in scientific applications, we now consider the fractional extension of Equation (1). The fractional version of the FitzHugh–Nagumo equation is derived from the well-known equation by replacing the first-order time derivative with an arbitrary-order derivative in the Caputo sense. This fractional model of FitzHugh–Nagumo Equation (1) can be expressed as follows:

$$u_t^\alpha = u_{xx} + u(u-\beta)(1-u), \quad t > 0,\ x \in \Omega, \tag{2}$$

with initial conditions (ICs) and boundary conditions (BCs)

$$\begin{cases} u(0,x) = u_0(x), & x \in \Omega, \\ u(t,a) = u_1(t), \quad \text{and} \quad u(t,b) = u_2(t), & x \in \partial\Omega, \quad t > 0, \end{cases} \tag{3}$$

where u is a function of both t and x, i.e., $u = u(t,x)$; β is an arbitrary constant; Ω represents the domain; and $\partial\Omega$ denotes the boundary of the domain. The time domain is defined as $t \in [0, t_{max}]$, where t_{max} is a finite real number representing the final time. The functions $u_0(x)$, $u_1(t)$, and $u_2(t)$ are known continuous functions. From Equation (2), it is important to observe that

1. When $\beta = -1$, then Equation (2) converts into the well-known Newell–Whitehead equation
$$u_t^\alpha = u_{xx} + u(u+1)(1-u), \quad t > 0,\ x \in \Omega. \tag{4}$$
2. When $\beta = 1$, then Equation (2) converts into the nonlinear FitzHugh–Nagumo equation
$$u_t^\alpha = u_{xx} + u(u-1)(1-u), \quad t > 0,\ x \in \Omega. \tag{5}$$
3. When $\beta = 0$, then Equation (2) converts into Fisher's equation
$$u_t^\alpha = u_{xx} + u^2(1-u), \quad t > 0,\ x \in \Omega. \tag{6}$$

Recent scientific research has involved a comprehensive exploration of the FitzHugh–Nagumo equation, employing a variety of analytical, numerical, and semianalytical methods to obtain both exact and approximate solutions. For instance, Kumar et al. [24] conducted a numerical investigation of the FitzHugh–Nagumo equation, utilizing a combination of the q-homotopy analysis approach and the Laplace transform method. Patel and Patel [25] examined the FitzHugh–Nagumo equation by applying the fractional reduced differential transform method (FRDTM). Abdel-Aty et al. [26] studied the time-fractional FitzHugh–Nagumo equation, both computationally and numerically, employing the improved Riccati expansion method and the B-spline method with a focus on the Atangana–Baleanu derivative. Additionally, Prakash and Kaur [27] explored the fractional model of the FitzHugh–Nagumo equation, which is relevant to the transmission of nerve impulses. They developed a reliable and computationally effective numerical scheme that combines the homotopy perturbation method with the Laplace transform approach. Lastly, Deniz [28] investigated the modified fractional version of the FitzHugh–Nagumo equation using the optimal perturbation iteration method.

Over the past decade, mesh-free methods using radial basis functions (RBFs) have gained significant prominence. This surge in interest is attributed to the challenges associated with classical numerical methods, such as the finite difference method, finite element method, and finite volume method, especially when dealing with two- or three-dimensional problems that require mesh generation. In 1990, Kansa introduced a technique for solving PDEs through the collocation method employing RBFs [29]. This approach involves approximating the solution using RBFs, and the collocation method is used to compute the unknown coefficients. The RBFs commonly used in the literature for solving PDEs include Hardy's multiquadric (MQ), Duchon's thin plate splines (TPSs), Gaussians (GS), inverse multiquadric (IMQ), and inverse quadric (IQ). The existence, uniqueness, and convergence of the RBF-based technique have been discussed by Franke and Schaback [30], Madych and Nelson [31], and Micchelli [32]. Kansa presented the initial concept of using RBFs to solve PDEs, and Golberg et al. [33] later refined it. In the context of solving PDEs, these RBFs have a shape parameter that can be adjusted to produce the best accurate results.

One of the main challenges associated with the RBF collocation method, as reported in the literature, is the dense and ill-conditioned nature of the system matrix that arises during the collocation process. This ill conditioning typically arises from a large number of nodes or an inappropriate choice of the shape parameter. However, various remedies for this issue have been proposed, including the contour-Padé algorithm, RBF-QR algorithm, extended precision arithmetic, and Hilbert–Schmidt decomposition, among others [34–36].

The main objective of this study is to compute a numerical solution for FitzHugh–Nagumo Equations (2) and (3) using the RBF collocation method. The structure of the paper is as follows: The methodology and stability analysis for Equations (2) and (3) are described in Section 2. Section 3 presents a number of examples and related discussions in order to validate the suggested methodology. Finally, in Section 4, a brief conclusion summarizes the study's important findings and contributions.

2. Methodology

The suggested meshless technique for solving FitzHugh–Nagumo Equations (2) and (3) will be discussed in this part along with its methodology. We present the notation to streamline our conversation: $\mathrm{u}^n = \mathrm{u}(\mathrm{t}_n, \mathrm{x})$, where $\mathrm{t}_n = n\delta\mathrm{t}|_{n=0}^{\mathrm{M}}$. Here, $\delta\mathrm{t} = \mathrm{t}_{max}/\mathrm{M}$ represents the time-step size, and $\mathrm{h} = 1/\mathrm{N}$ is the space-step size, where N and M are the number of points in the intervals $[\mathrm{a}, \mathrm{b}]$ and $[0, \mathrm{t}_{\max}]$, respectively.

The time-fractional derivative in Equation (2) uses the Caputo fractional partial derivative of order $\alpha \in (0, 1)$, defined as [16]

$$\frac{\partial^{\alpha}\mathrm{u}}{\partial\mathrm{t}^{\alpha}} = \frac{1}{\Gamma(1-\alpha)}\int_0^{\mathrm{t}} \frac{\partial\mathrm{u}}{\partial\mathrm{s}}(\mathrm{t}-\mathrm{s})^{-\alpha} d\mathrm{s}.$$

2.1. Time-Fractional Derivative Approximation

In Equation (2), the temporal part is discretized using the method described in [37] as follows:

$$\begin{aligned}\frac{\partial^{\alpha}\mathrm{u}^{n+1}}{\partial \mathrm{t}^{\alpha}} =& \frac{(\delta \mathrm{t})^{-\alpha}}{\Gamma(2-\alpha)}\sum_{k=0}^{n}\left(\mathrm{u}^{n+1-k}-\mathrm{u}^{n-k}\right)\left((k+1)^{1-\alpha}-(k)^{1-\alpha}\right)+\mathcal{O}(\delta \mathrm{t}^{2-\alpha}) \\ =& \ell_{\alpha}^{*}\left(\mathrm{u}^{n+1}-\mathrm{u}^{n}\right)+\mathfrak{B}^{n}+\mathcal{O}(\delta \mathrm{t}^{2-\alpha}),\end{aligned}$$

where

$$\mathfrak{B}^{n}=\ell_{\alpha}^{*}\sum_{k=1}^{n}\ell_{\alpha}^{**}(k)\left(\mathrm{u}^{n+1-k}-\mathrm{u}^{n-k}\right)$$

and

$$\ell_{\alpha}^{*}=\frac{(\delta \mathrm{t})^{-\alpha}}{\Gamma(2-\alpha)}, \quad \ell_{\alpha}^{**}(k)=(k+1)^{1-\alpha}-(k)^{1-\alpha}.$$

It is important to observe that $\mathfrak{B}^{n}=0$ whenever $n=0$. With this consideration, the discretization formula can be expressed as follows:

$$\frac{\partial^{\alpha}\mathrm{u}^{n+1}}{\partial \mathrm{t}^{\alpha}}=\begin{cases}\ell_{\alpha}^{*}\left(\mathrm{u}^{n+1}-\mathrm{u}^{n}\right)+\mathfrak{B}^{n}+\mathcal{O}(\delta \mathrm{t}^{2-\alpha}), & \alpha\in(0,1),\\ \dfrac{\mathrm{u}^{n+1}-\mathrm{u}^{n}}{\delta \mathrm{t}}+\mathcal{O}(\delta \mathrm{t}), & \alpha=1.\end{cases} \tag{7}$$

2.2. The θ-Weighted Scheme

Utilizing Equation (7) in conjunction with the θ-weighted scheme and neglecting the error term, we can express Equation (2) in their time-discretized form as follows:

$$\begin{aligned}&\ell_{\alpha}^{*}\mathrm{u}^{n+1}-\theta\left(\mathrm{u}_{\mathrm{xx}}^{n+1}-\left(\mathrm{u}^{n+1}\right)^{3}+(1+\beta)\left(\mathrm{u}^{n+1}\right)^{2}-\beta\mathrm{u}^{n+1}\right)\\ &=\ell_{\alpha}^{*}\mathrm{u}^{n}-(\theta-1)\left(\mathrm{u}_{\mathrm{xx}}^{n}-(\mathrm{u}^{n})^{3}+(1+\beta)(\mathrm{u}^{n})^{2}-\beta\mathrm{u}^{n}\right)-\mathfrak{B}^{n}.\end{aligned} \tag{8}$$

The nonlinear terms in Equation (8) can be linearized using the following approach:

$$\begin{cases}\left(\mathrm{u}^{n+1}\right)^{3}=3(\mathrm{u}^{n})^{2}\mathrm{u}^{n+1}-2(\mathrm{u}^{n})^{3},\\ \left(\mathrm{u}^{n+1}\right)^{2}=2\mathrm{u}^{n}\mathrm{u}^{n+1}-(\mathrm{u}^{n})^{2}.\end{cases} \tag{9}$$

By substituting the values from Equation (9) into Equation (8), the following expressions can be obtained after simplification:

$$\nu_{1}^{n}\mathrm{u}^{n+1}-\theta\mathrm{u}_{\mathrm{xx}}^{n+1}=\nu_{2}^{n}\mathrm{u}^{n}+(1-\theta)\mathrm{u}_{\mathrm{xx}}^{n}-\mathfrak{B}^{n}, \tag{10}$$

where

$$\nu_{1}^{n}=\ell_{\alpha}^{*}+\theta\left(\beta-2(1+\beta)\mathrm{u}^{n}+3(\mathrm{u}^{n})^{2}\right) \quad \text{and} \quad \nu_{2}^{n}=\ell_{\alpha}^{*}+\beta(\theta-1)+(3\theta-1)(\mathrm{u}^{n})^{2}+(1+\beta-2\theta(1+\beta))\mathrm{u}^{n}.$$

2.3. Radial Basis Function Approximation Scheme

Now, we move on to approximating the spatial component using RBFs and the collocation method. To do this, the collocation points are taken as $\{\mathrm{x}_i\}_{i=1}^{\mathrm{N}}$. Consequently, we can represent the solution at interior points by employing RBFs denoted as $\phi_{ij}=\phi(\|\mathrm{x}_i-\mathrm{x}_j\|)$ in the following manner:

$$\mathrm{u}^{n+1}=\sum_{j=1}^{\mathrm{N}}\lambda_{j}^{n+1}\phi_{ij}=\Phi\urcorner^{n+1}, \quad i=2,\dots,\mathrm{N}-1, \tag{11}$$

where $\daleth^{n+1} = [\lambda_1^{n+1}, \ldots, \lambda_N^{n+1}]^T$ represents a vector of unknown coefficients at the $(n+1)^{th}$ time level. $\Phi = [\phi_{ij}]_{1\leqslant i,j\leqslant N}$ is the matrix of RBFs, and $\|\cdot\|$ denotes the Euclidean norm. The boundary conditions (3) are approximated as follows:

$$\sum_{j=1}^{N} \lambda_j^{n+1}\phi_{1j} = u_1^{n+1} \quad \text{and} \quad \sum_{j=1}^{N} \lambda_j^{n+1}\phi_{Nj} = u_2^{n+1}. \tag{12}$$

Furthermore, the spatial derivative at the interior points $x \in \Omega$ are given as follows:

$$u_{xx}^{n+1} = \Phi_{xx}\daleth^{n+1}. \tag{13}$$

By substituting Equations (11)–(13) into Equation (10) and performing simplifications, we arrive at the following equation:

$$\mathbf{A}\daleth^{n+1} = \mathbf{B}\daleth^{n} + \mathbf{Z}^{n+1}, \tag{14}$$

where

$$\mathbf{A} = \begin{cases} \nu_1^n[\Phi]_{ij} - \theta[\Phi_{xx}]_{ij}, & x_i \in \Omega, \\ [\Phi]_{ij}, & x_i \in \partial\Omega, \end{cases}$$

$$\mathbf{B} = \begin{cases} \nu_2^n[\Phi]_{ij} + (1-\theta)[\Phi_{xx}]_{ij}, & x_i \in \Omega, \\ 0, & x_i \in \partial\Omega, \end{cases}$$

$$\mathbf{Z} = \begin{cases} -\mathfrak{B}^n, & x_i \in \Omega, \\ \mathfrak{C}^{n+1}, & x_i \in \partial\Omega, \end{cases}$$

where $\mathfrak{C}^{n+1} = [u_1^{n+1}, 0, \cdots, 0, u_2^{n+1}]^T$. Now Equation (14) implies that

$$\daleth^{n+1} = \mathbf{A}^{-1}\mathbf{B}\daleth^{n} + \mathbf{A}^{-1}\mathbf{Z}^{n+1}. \tag{15}$$

From Equations (11) and (15), it follows that

$$u^{n+1} = \Phi\mathbf{A}^{-1}\mathbf{B}\Phi^{-1}u^n + \Phi\mathbf{A}^{-1}\mathbf{Z}^{n+1}. \tag{16}$$

The numerical solution at any given time level n using scheme (16) can be obtained. We initialize the initial value u^0 by incorporating the initial condition $u(0,x) = u_0(x)$. In the subsequent section, stability analysis of scheme (16) will be discussed.

2.4. Stability

To examine stability, we employ an approach outlined in [38]. For the error vector $\mathbb{E}$ defined as

$$\mathbb{E} = u_{exact} - u_{approx},$$

the relation in (16) can be expressed as

$$\mathbb{E}^{n+1} = \wp\mathbb{E}^n,$$

where $\wp = \Phi\mathbf{A}^{-1}\mathbf{B}\Phi^{-1}$ represents the amplification matrix. According to the Lax–Richtmyer criterion of stability, the present method can be considered stable if

$$\|\wp\| \leqslant 1.$$

It is important to note that the inequality

$$\rho(\wp) \leqslant \|\wp\|$$

always holds, where $\rho(\wp)$ represents the spectral radius of the matrix $\wp$.

3. Computational Results and Discussion

In this section, the implementation of the method for solving FitzHugh–Nagumo Equations (2) and (3) has been presented. Computer simulations have been carried out via MATLAB R2020a on a PC with the following configuration: processor: Intel (R) Core (TM) i7-4790 CPU @ 3.60 GHz 3.60 GHz, RAM 8.00 GB, and system type: 64-bit operating system, x64-based processor. The accuracy and efficiency of the method are assessed using the following error norms:

$$L_2 = \left[h \sum_{i=1}^{N} (u_{exact} - u_{approx})^2 \right]^{1/2}, \quad L_\infty = \max_i |u_{exact} - u_{approx}|,$$
$$L_{rms} = \left[\frac{1}{N} \sum_{i=1}^{N} (u_{exact} - u_{approx})^2 \right]^{1/2}, \quad \text{Absolute error} = |u_{exact} - u_{approx}|.$$

For the solution of FitzHugh–Nagumo Equations (2) and (3), the following RBFs have been used:

- $MQ : \phi_{ij} = \sqrt{r_{ij}^2 + c^2}$;
- $IMQ : \phi_{ij} = \left(r_{ij}^2 + c^2\right)^{-1/2}$;
- $IQ : \phi_{ij} = \left(r_{ij}^2 + c^2\right)^{-1}$;
- $GS : \phi_{ij} = \exp(-c^2 r_{ij}^2)$,

where $c > 0$ represents the shape parameter and $r_{ij} = |x_i - x_j|_{1 \leqslant i,j \leqslant N}$.

Selection of Shape Parameter

Determining the optimal value for the shape parameter c can be a challenging task. The random selection of c can be a limitation since many researchers choose c using suboptimal criteria. Therefore, in this study, we employ the extended Rippa algorithm to select the optimal shape parameter. Rippa's algorithm, as described by Rippa [39], estimates the cost function based on the norm of the error vector, which can be either the L_2 or L_∞ norm. The parameter c that minimizes this cost function is deemed satisfactory, as it results in an approximation quality comparable to that achieved with the optimal c. We also provide plots illustrating the best-suited values of c obtained using this algorithm.

Example 1. *Let us consider FitzHugh–Nagumo Equations* (2) *and* (3) *with* $\beta = 1$. *The exact solution is given by [25]*

$$u(t,x) = \frac{1}{2} + \frac{1}{2}\tanh\left(\frac{\sqrt{2}x - t}{4}\right).$$

The ICs and BCs are derived from the exact solution within the domain $x \in [0,1]$. *The approximate solution is obtained using various RBFs, such as MQ, IMQ, IQ, and GS, with parameters* $N = 10$ *and* $\delta t = 0.1$ *for different values of* α *(0.25, 0.5, 0.75, and 1). The present method is examined, and the results are recorded in Tables 1 and 2 for various nodal points* (x_i, t_n). *The results are then compared with FRDTM. The comparison reveals that the present method produces good accuracy, specially for fractional order with the best results obtained using GS, MQ, IMQ, and IQ. Additionally, error norms at various time levels using the mentioned RBFs are dispatched in Tables 3 and 4.*

Furthermore, stability and error norm plots are displayed in Figure 1 for MQ, IMQ, IQ, and GS RBFs against the shape parameter. These plots clearly demonstrate that the present method fully satisfies the Lax–Richtmyer stability criterion. Surface plots in Figure 2 illustrate that the computed solutions using these RBFs closely match the exact solution. Absolute errors at various time levels for $\alpha = 1$ *are shown in Figure 3, indicating reasonable accuracy. A comparison between the exact* *and computed solutions at the final time level is presented in Figure 4, confirming the high accuracy of the present method. Finally, in Figures 5–8, absolute errors for different values of α's at various time levels are shown using MQ, IMQ, IQ, and GS, respectively.*

Table 1. Comparison of computed values of the present method solution with FRDTM using MQ, IMQ, IQ, and GS RBFs for $\alpha = 0.25, 0.5$, $\beta = 1$, $N = 10$, $\theta = 0.5$, and $\delta t = 0.1$ corresponds to Example 1.

(x, t)	Exact	$\alpha = 0.25$					$\alpha = 0.5$				
		[25]	MQ	IMQ	IQ	GS	[25]	MQ	IMQ	IQ	GS
			c = 6.824741	c = 8.12967	c = 5.34901	c = 0.251637		c = 5.8659	c = 6.88885	c = 5.18412	c = 0.25937
(0.1, 0.2)	0.492678	0.427418	0.492029	0.492126	0.492364	0.492466	0.454935	0.492344	0.492386	0.492489	0.492564
(0.1, 0.4)	0.467723	0.411555	0.467129	0.467083	0.467582	0.467632	0.429688	0.467279	0.467401	0.467571	0.467645
(0.1, 0.6)	0.442927	0.401291	0.443115	0.442313	0.442917	0.442952	0.410894	0.442364	0.442535	0.442858	0.442910
(0.1, 0.8)	0.418414	0.393583	0.418856	0.418114	0.418463	0.418448	0.395550	0.418125	0.418259	0.418442	0.418426
(0.3, 0.2)	0.528004	0.461640	0.526474	0.526698	0.527298	0.527493	0.489905	0.527223	0.527325	0.527585	0.527735
(0.3, 0.4)	0.503033	0.445267	0.501595	0.501492	0.502762	0.502797	0.464133	0.501982	0.502252	0.502729	0.502842
(0.3, 0.6)	0.478047	0.434619	0.478461	0.476553	0.478071	0.478089	0.444777	0.476697	0.477079	0.477948	0.477992
(0.3, 0.8)	0.453171	0.426595	0.454236	0.452429	0.453300	0.453249	0.428860	0.452424	0.452737	0.453293	0.453186
(0.5, 0.2)	0.563051	0.496159	0.561223	0.561488	0.562257	0.562434	0.524966	0.562128	0.562253	0.562589	0.562736
(0.5, 0.4)	0.538313	0.479367	0.536561	0.536435	0.538071	0.538014	0.498899	0.537055	0.537363	0.538023	0.538083
(0.5, 0.6)	0.513385	0.468375	0.513874	0.511551	0.513484	0.513427	0.479131	0.511752	0.512181	0.513354	0.513312
(0.5, 0.8)	0.488390	0.460051	0.489708	0.487477	0.488573	0.488485	0.462744	0.487455	0.487818	0.488617	0.488400
(0.7, 0.2)	0.597480	0.530655	0.595947	0.596167	0.596862	0.596963	0.559780	0.596717	0.596823	0.597129	0.597225
(0.7, 0.4)	0.573214	0.513551	0.571727	0.571609	0.573089	0.572956	0.533657	0.572160	0.572409	0.573040	0.573026
(0.7, 0.6)	0.548590	0.502269	0.549021	0.547016	0.548741	0.548627	0.513645	0.547210	0.547543	0.548648	0.548530
(0.7, 0.8)	0.523726	0.493674	0.524882	0.522951	0.523912	0.523812	0.496910	0.522935	0.523224	0.523996	0.523734
(0.9, 0.2)	0.630974	0.564813	0.630322	0.630415	0.630735	0.630756	0.594013	0.630655	0.630700	0.630843	0.630870
(0.9, 0.4)	0.607400	0.547522	0.606766	0.606706	0.607385	0.607291	0.568079	0.606954	0.607057	0.607361	0.607325
(0.9, 0.6)	0.583315	0.536019	0.583518	0.582633	0.583413	0.583335	0.548003	0.582725	0.582855	0.583381	0.583293
(0.9, 0.8)	0.558825	0.527198	0.559346	0.558498	0.558922	0.558867	0.531062	0.558499	0.558612	0.558979	0.558831

Table 2. Comparison of computed values of the present method solution with FRDTM using MQ, IMQ, IQ, and GS RBFs for $\alpha = 0.75, 1$, $\beta = 1$, $N = 10$, $\theta = 0.5$, and $\delta t = 0.1$ corresponds to Example 1.

(x, t)	Exact	$\alpha = 0.75$					$\alpha = 1$				
		[25]	MQ	IMQ	IQ	GS	[25]	MQ	IMQ	IQ	GS
			c = 5.80145	c = 4.48635	c = 5.38471	c = 0.26237		c = 6.78326	c = 7.23608	c = 7.88039	c = 0.16625
(0.1, 0.2)	0.492678	0.477029	0.492540	0.492594	0.492594	0.492630	0.492678	0.492674	0.492676	0.492674	0.492666
(0.1, 0.4)	0.467723	0.449555	0.467487	0.467619	0.467623	0.467672	0.467722	0.467706	0.467716	0.467707	0.467642
(0.1, 0.6)	0.442927	0.425857	0.442690	0.442835	0.442856	0.442912	0.442927	0.442909	0.442918	0.442905	0.442841
(0.1, 0.8)	0.418414	0.404564	0.418328	0.418368	0.418407	0.418433	0.418416	0.418407	0.418406	0.418399	0.418391
(0.3, 0.2)	0.528004	0.512307	0.527682	0.527809	0.527819	0.527892	0.528003	0.527996	0.528000	0.527994	0.527975
(0.3, 0.4)	0.503033	0.484582	0.502475	0.502807	0.502828	0.502912	0.503030	0.502996	0.503019	0.502999	0.502881
(0.3, 0.6)	0.478047	0.460446	0.477457	0.477869	0.477926	0.478004	0.478035	0.478003	0.478026	0.477996	0.477887
(0.3, 0.8)	0.453171	0.438573	0.452937	0.453093	0.453193	0.453211	0.453136	0.453156	0.453153	0.453136	0.453114
(0.5, 0.2)	0.563051	0.547464	0.562671	0.562826	0.562848	0.562922	0.563051	0.563043	0.563047	0.563041	0.563015
(0.5, 0.4)	0.538313	0.519760	0.537643	0.538070	0.53811	0.538172	0.538308	0.53827	0.538298	0.538274	0.538165
(0.5, 0.6)	0.513385	0.495415	0.512658	0.513228	0.513305	0.513335	0.513362	0.513331	0.513361	0.513326	0.513249
(0.5, 0.8)	0.488390	0.473159	0.488089	0.488345	0.488474	0.488438	0.488322	0.488375	0.488370	0.488348	0.488328
(0.7, 0.2)	0.597480	0.582153	0.597165	0.597300	0.597326	0.597377	0.597479	0.597474	0.597477	0.597471	0.597446
(0.7, 0.4)	0.573214	0.554743	0.572650	0.573038	0.573084	0.573102	0.573207	0.573178	0.573202	0.573181	0.573113
(0.7, 0.6)	0.548590	0.530429	0.547972	0.548512	0.548585	0.548554	0.548558	0.548544	0.548571	0.548541	0.548522
(0.7, 0.8)	0.523726	0.508002	0.523469	0.523735	0.523852	0.523770	0.523629	0.523715	0.523709	0.523691	0.523680
(0.9, 0.2)	0.630974	0.616050	0.630841	0.630902	0.630917	0.630933	0.630973	0.630971	0.630972	0.630970	0.630957
(0.9, 0.4)	0.607400	0.589194	0.607160	0.607341	0.607365	0.607357	0.607392	0.607384	0.607395	0.607386	0.607368
(0.9, 0.6)	0.583315	0.565149	0.583053	0.583308	0.583343	0.583305	0.583277	0.583296	0.583307	0.583294	0.583305
(0.9, 0.8)	0.558825	0.542773	0.558721	0.558852	0.558906	0.558848	0.558707	0.558822	0.558818	0.558811	0.558809

Table 3. Error norms at various time levels using MQ, IMQ, IQ, and GS RBFs for $\alpha = 0.25, 0.5$, $\beta = 1$, $N = 10$, $\theta = 0.5$, and $\delta t = 0.1$ corresponds to Example 1.

RBFs	**t**	$\boldsymbol{\alpha = 0.25}$			$\boldsymbol{\alpha = 0.5}$		
		L_2	L_∞	L_{rms}	L_2	L_∞	L_{rms}
MQ		c = 6.824741			c = 5.8659		
	0.2	1.331×10^{-3}	1.828×10^{-3}	1.270×10^{-3}	6.715×10^{-4}	9.231×10^{-4}	6.402×10^{-4}
	0.4	1.272×10^{-3}	1.752×10^{-3}	1.213×10^{-3}	9.153×10^{-4}	1.259×10^{-3}	8.727×10^{-4}
	0.6	3.663×10^{-4}	4.893×10^{-4}	3.493×10^{-4}	1.187×10^{-3}	1.633×10^{-3}	1.132×10^{-3}
	0.8	9.663×10^{-4}	1.318×10^{-3}	9.214×10^{-4}	6.701×10^{-4}	9.350×10^{-4}	6.389×10^{-4}
	1	4.238×10^{-6}	7.006×10^{-6}	4.041×10^{-6}	7.414×10^{-6}	1.297×10^{-5}	7.069×10^{-6}
IMQ		c = 8.12967			c = 6.88885		
	0.2	1.138×10^{-3}	1.563×10^{-3}	1.085×10^{-3}	5.811×10^{-4}	7.983×10^{-4}	5.541×10^{-4}
	0.4	1.368×10^{-3}	1.879×10^{-3}	1.304×10^{-3}	6.897×10^{-4}	9.504×10^{-4}	6.576×10^{-4}
	0.6	1.334×10^{-3}	1.835×10^{-3}	1.272×10^{-3}	8.769×10^{-4}	1.204×10^{-3}	8.360×10^{-4}
	0.8	6.601×10^{-4}	9.134×10^{-4}	6.294×10^{-4}	4.089×10^{-4}	5.721×10^{-4}	3.899×10^{-4}
	1	1.199×10^{-6}	1.851×10^{-6}	1.143×10^{-6}	5.718×10^{-6}	9.971×10^{-6}	5.452×10^{-6}
IQ		c = 5.34901			c = 5.18412		
	0.2	5.766×10^{-4}	7.940×10^{-4}	5.498×10^{-4}	3.359×10^{-4}	4.623×10^{-4}	3.202×10^{-4}
	0.4	1.825×10^{-4}	2.724×10^{-4}	1.740×10^{-4}	2.147×10^{-4}	3.145×10^{-4}	2.047×10^{-4}
	0.6	9.193×10^{-5}	1.510×10^{-4}	8.765×10^{-5}	6.746×10^{-5}	1.006×10^{-4}	6.432×10^{-5}
	0.8	1.387×10^{-4}	1.929×10^{-4}	1.322×10^{-4}	1.804×10^{-4}	2.700×10^{-4}	1.720×10^{-4}
	1	5.465×10^{-6}	8.804×10^{-6}	5.211×10^{-6}	3.988×10^{-6}	6.707×10^{-6}	3.803×10^{-6}
GS		c = 0.251637			c = 0.25937		
	0.2	4.473×10^{-4}	6.166×10^{-4}	4.265×10^{-4}	2.279×10^{-4}	3.146×10^{-4}	2.173×10^{-4}
	0.4	2.152×10^{-4}	2.992×10^{-4}	2.052×10^{-4}	1.651×10^{-4}	2.302×10^{-4}	1.574×10^{-4}
	0.6	3.447×10^{-5}	4.323×10^{-5}	3.286×10^{-5}	5.054×10^{-5}	7.298×10^{-5}	4.819×10^{-5}
	0.8	7.107×10^{-5}	9.455×10^{-5}	6.776×10^{-5}	1.058×10^{-5}	1.617×10^{-5}	1.009×10^{-5}
	1	4.706×10^{-6}	7.906×10^{-6}	4.487×10^{-6}	4.625×10^{-6}	8.048×10^{-6}	4.410×10^{-6}

Table 4. Error norms at various time levels using MQ, IMQ, IQ, and GS RBFs for $\alpha = 0.75, 1$, $\beta = 1$, $N = 10$, $\theta = 0.5$, and $\delta t = 0.1$ corresponds to Example 1.

RBFs	**t**	$\boldsymbol{\alpha = 0.75}$			$\boldsymbol{\alpha = 1}$		
		L_2	L_∞	L_{rms}	L_2	L_∞	L_{rms}
MQ		c = 5.80145			c = 6.78326		
	0.2	2.769×10^{-4}	3.802×10^{-4}	2.640×10^{-4}	5.932×10^{-6}	8.084×10^{-6}	5.656×10^{-6}
	0.4	4.878×10^{-4}	6.702×10^{-4}	4.651×10^{-4}	3.153×10^{-5}	4.263×10^{-5}	3.006×10^{-5}
	0.6	5.258×10^{-4}	7.275×10^{-4}	5.013×10^{-4}	3.904×10^{-5}	5.393×10^{-5}	3.722×10^{-5}
	0.8	2.143×10^{-4}	3.014×10^{-4}	2.044×10^{-4}	1.143×10^{-5}	1.609×10^{-5}	1.090×10^{-5}
	1	4.401×10^{-6}	6.944×10^{-6}	4.196×10^{-6}	7.107×10^{-7}	1.410×10^{-6}	6.776×10^{-7}
IMQ		c = 4.48635			c = 7.23608		
	0.2	1.630×10^{-4}	2.249×10^{-4}	1.554×10^{-4}	2.886×10^{-6}	3.898×10^{-6}	2.751×10^{-6}
	0.4	1.759×10^{-4}	2.466×10^{-4}	1.678×10^{-4}	1.103×10^{-5}	1.490×10^{-5}	1.052×10^{-5}
	0.6	1.191×10^{-4}	1.785×10^{-4}	1.135×10^{-4}	1.739×10^{-5}	2.373×10^{-5}	1.658×10^{-5}
	0.8	4.659×10^{-5}	7.766×10^{-5}	4.442×10^{-5}	1.510×10^{-5}	2.085×10^{-5}	1.440×10^{-5}
	1	4.166×10^{-6}	6.616×10^{-6}	3.972×10^{-6}	4.264×10^{-7}	6.996×10^{-7}	4.065×10^{-7}

Table 4. *Cont.*

RBFs	t	$\alpha = 0.75$			$\alpha = 1$		
		L_2	L_∞	L_{rms}	L_2	L_∞	L_{rms}
		c = 5.38471			c = 7.88039		
IQ	0.2	1.476×10^{-4}	2.032×10^{-4}	1.407×10^{-4}	7.689×10^{-6}	1.021×10^{-5}	7.331×10^{-6}
	0.4	1.489×10^{-4}	2.155×10^{-4}	1.420×10^{-4}	2.877×10^{-5}	3.894×10^{-5}	2.743×10^{-5}
	0.6	7.313×10^{-5}	1.212×10^{-4}	6.972×10^{-5}	4.352×10^{-5}	5.947×10^{-5}	4.149×10^{-5}
	0.8	7.707×10^{-5}	1.263×10^{-4}	7.349×10^{-5}	3.045×10^{-5}	4.238×10^{-5}	2.903×10^{-5}
	1	1.266×10^{-6}	2.428×10^{-6}	1.207×10^{-6}	5.121×10^{-7}	8.217×10^{-7}	4.883×10^{-7}
		c = 0.26237			c = 0.16625		
GS	0.2	9.327×10^{-5}	1.287×10^{-4}	8.893×10^{-5}	2.726×10^{-5}	3.641×10^{-5}	2.599×10^{-5}
	0.4	1.016×10^{-4}	1.413×10^{-4}	9.682×10^{-5}	1.115×10^{-4}	1.571×10^{-4}	1.063×10^{-4}
	0.6	3.468×10^{-5}	5.034×10^{-5}	3.306×10^{-5}	1.060×10^{-4}	1.599×10^{-4}	1.011×10^{-4}
	0.8	3.649×10^{-5}	4.743×10^{-5}	3.479×10^{-5}	4.430×10^{-5}	6.206×10^{-5}	4.224×10^{-5}
	1	2.129×10^{-6}	2.664×10^{-6}	2.030×10^{-6}	5.164×10^{-6}	6.820×10^{-6}	4.924×10^{-6}

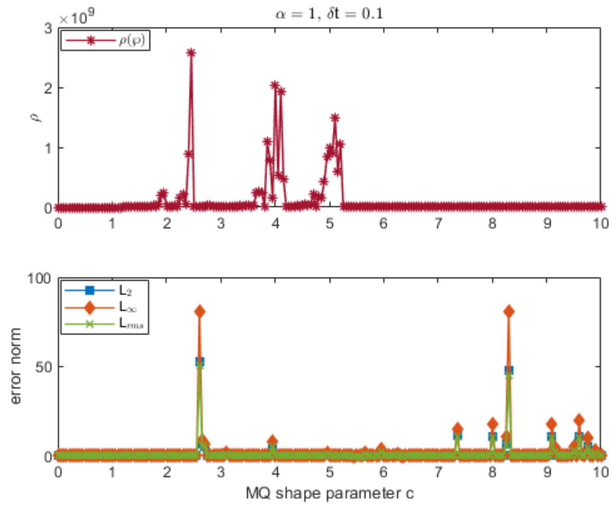

(**a**) Error norms and spectral radius using MQ

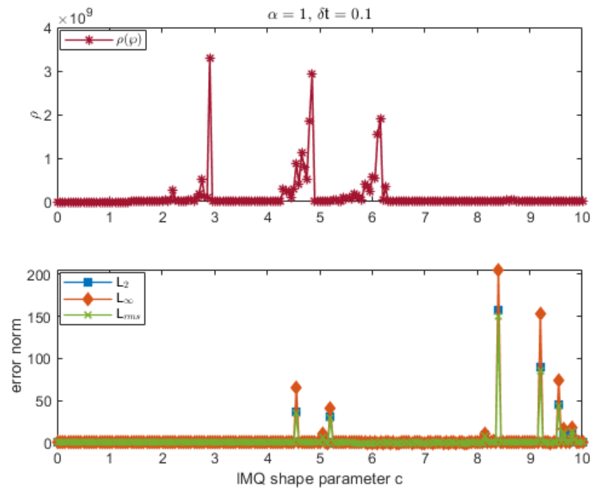

(**b**) Error norms and spectral radius using IMQ

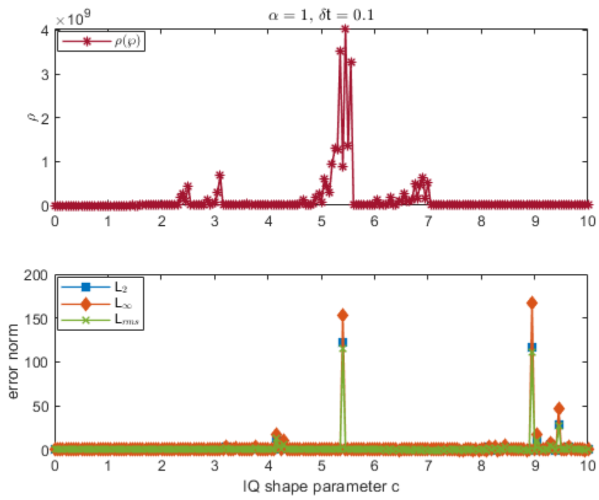

(**c**) Error norms and spectral radius against IQ

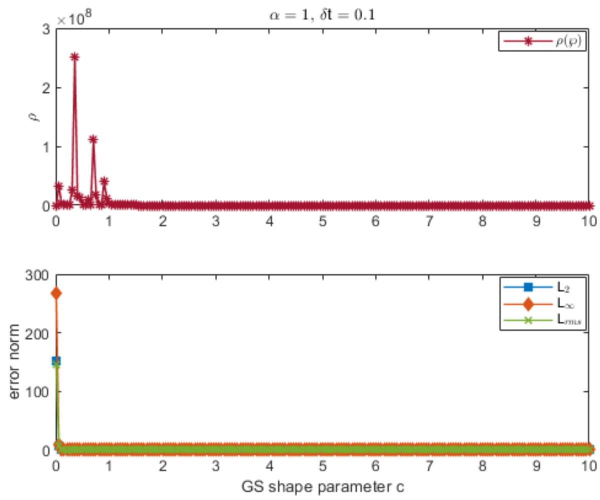

(**d**) Error norms and spectral radius using GS

Figure 1. Error norms and spectral radius correspond to Example 1 when N = M = 10, $\theta = 0.5$ using MQ, IMQ, IQ, and GS RBFs.

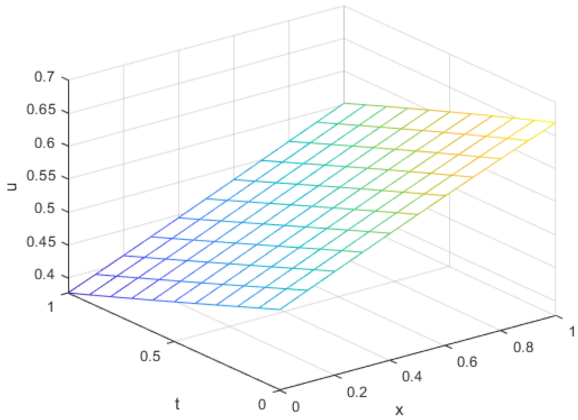

(**a**) Exact solution

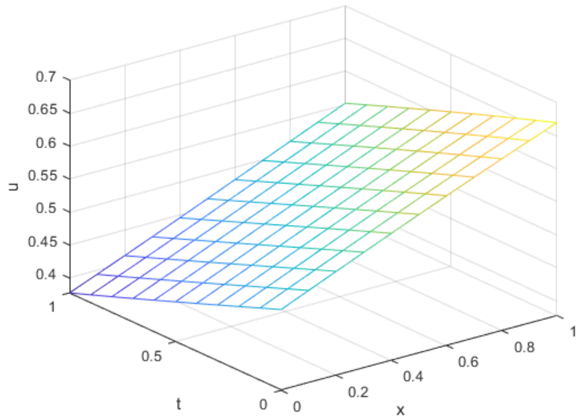

(**b**) Computed solution using MQ

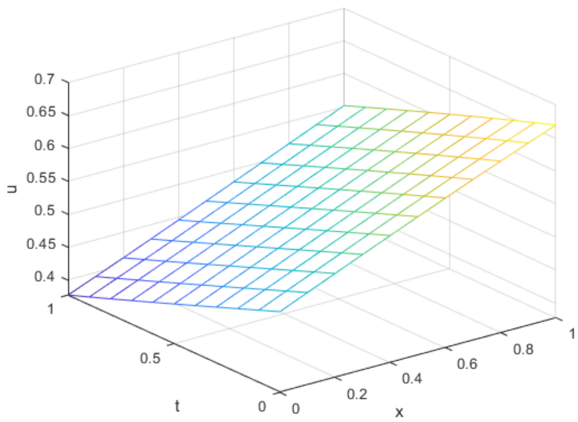

(**c**) Computed solution using IMQ

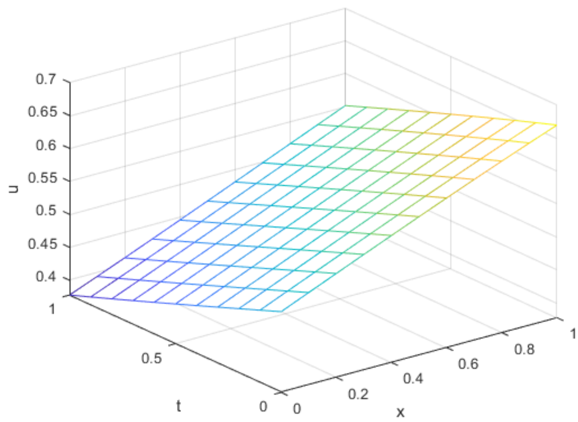

(**d**) Computed solution against IQ

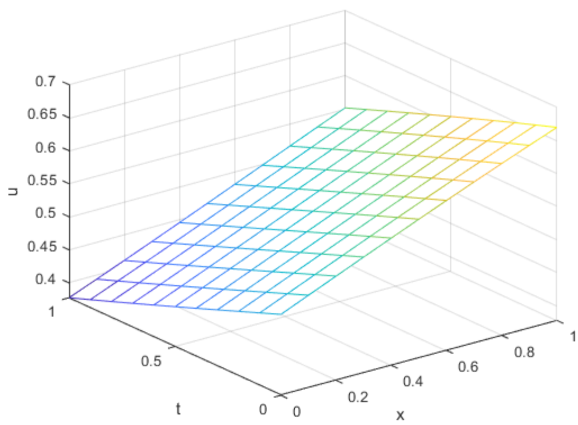

(**e**) Computed solution using GS

Figure 2. Exact vs. computed solution corresponds to Example 1 when $N = M = 10$, $\alpha = 1$ using MQ, IMQ, IQ, and GS RBFs.

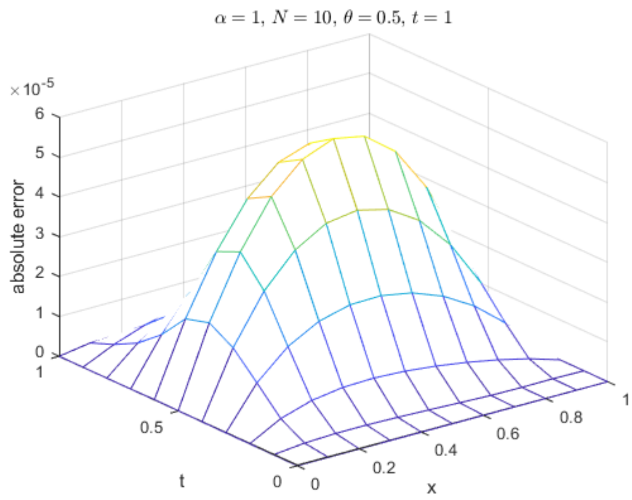

(**a**) Absolute error using MQ

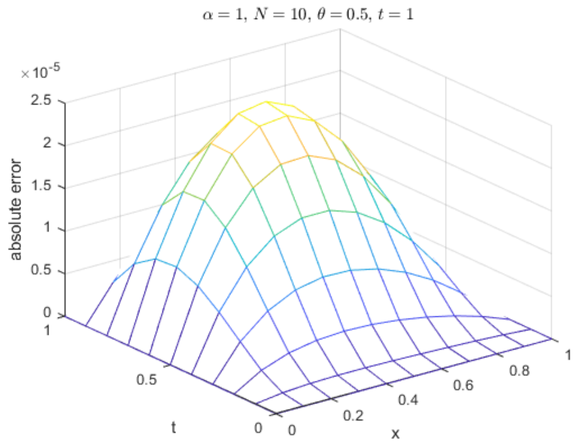

(**b**) Absolute error using IMQ

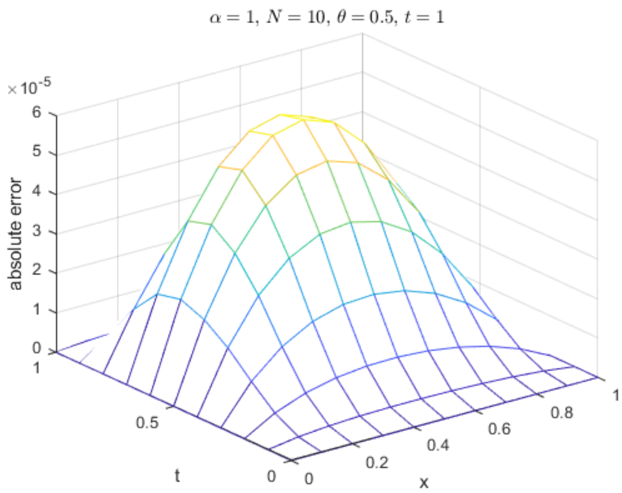

(**c**) Absolute error against IQ

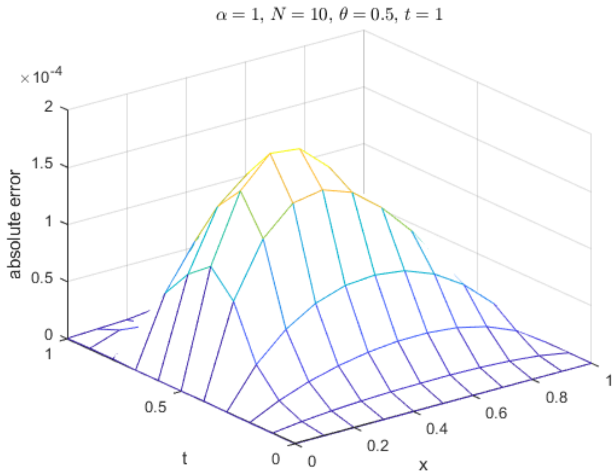

(**d**) Absolute error using GS

Figure 3. Absolute error of MQ, IMQ, IQ, and GS at t = 1 corresponds to Example 1.

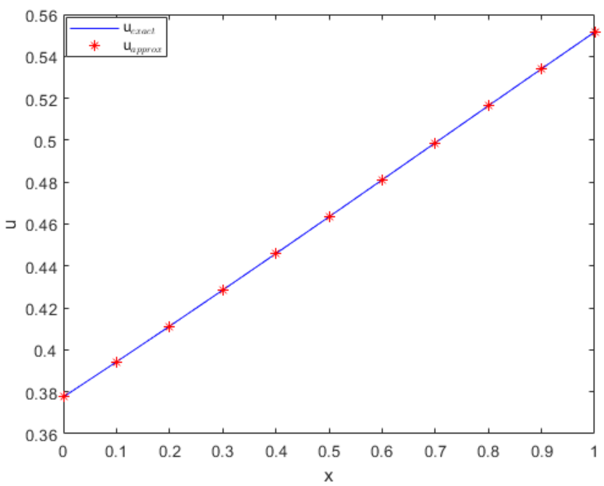

(**a**) Exact vs. numerical using MQ

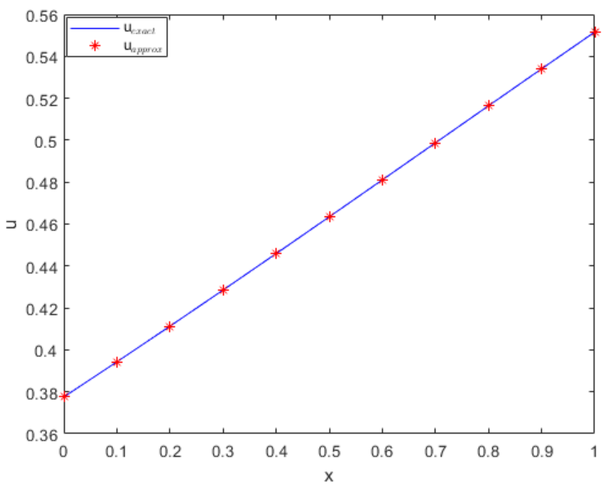

(**b**) Exact vs. numerical using IMQ

Figure 4. *Cont.*

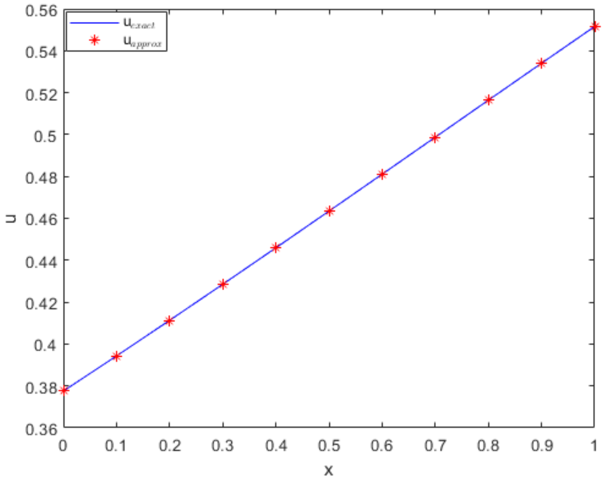

(**c**) Exact vs. numerical against IQ

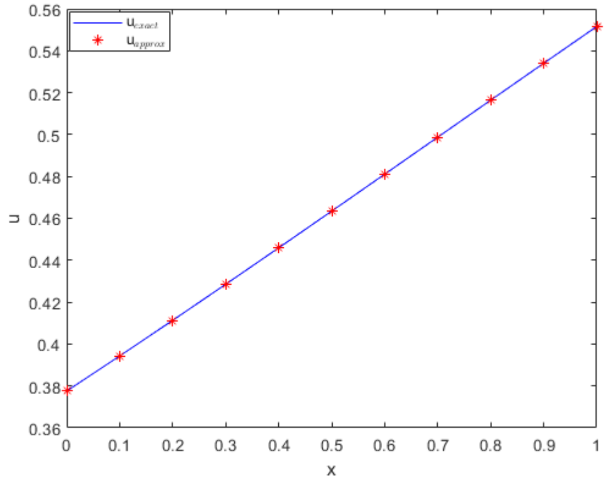

(**d**) Exact vs. numerical using GS

Figure 4. Comparison of exact and computed solution corresponds to Example 1 at t = 1 and $\alpha = 1$ using MQ, IMQ, IQ, and GS RBFs.

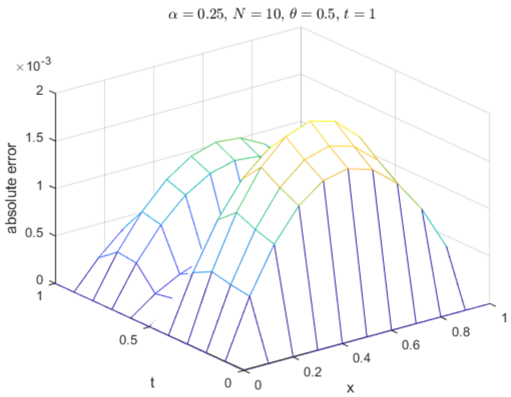

(**a**) Absolute error

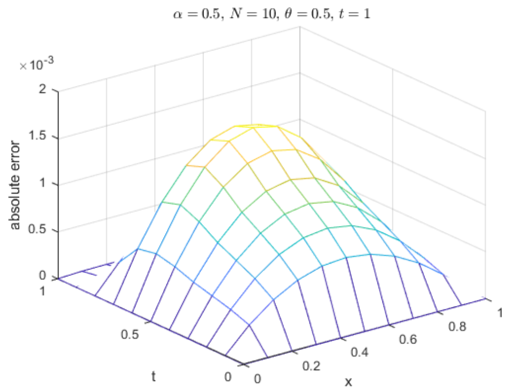

(**b**) Absolute error

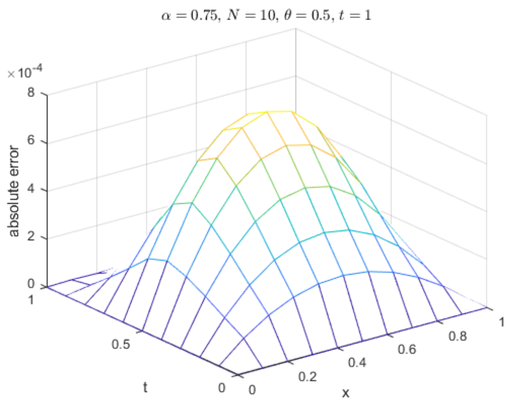

(**c**) Absolute error

Figure 5. Absolute errors for Example 1 with different values of α's using MQ RBF.

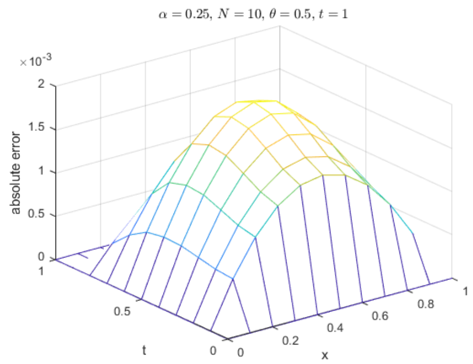

(**a**) Absolute error

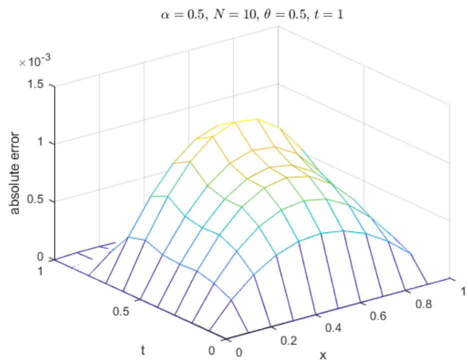

(**b**) Absolute error

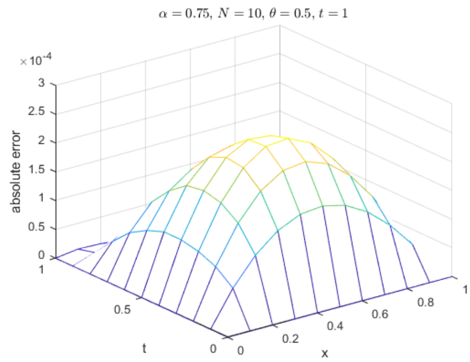

(**c**) Absolute error

Figure 6. Absolute errors for Example 1 with different values of α's using IMQ RBF.

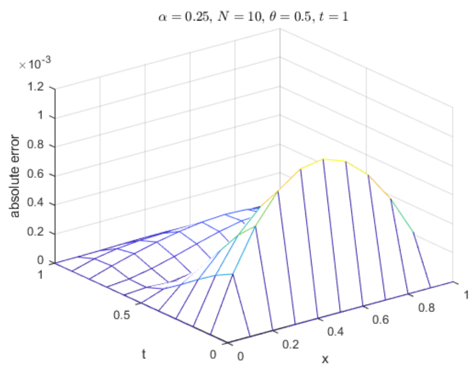

(**a**) Absolute error

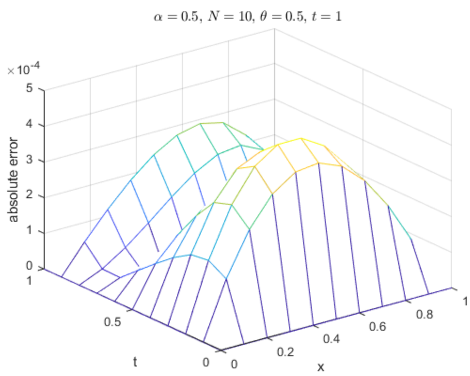

(**b**) Absolute error

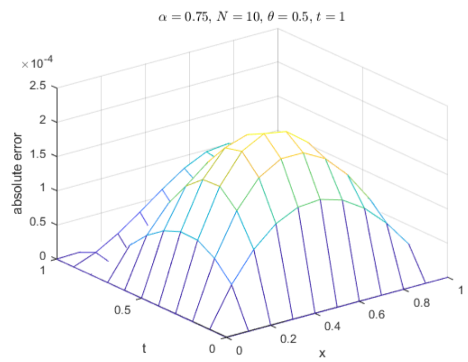

(**c**) Absolute error

Figure 7. Absolute errors for Example 1 with different values of α's using IQ RBF.

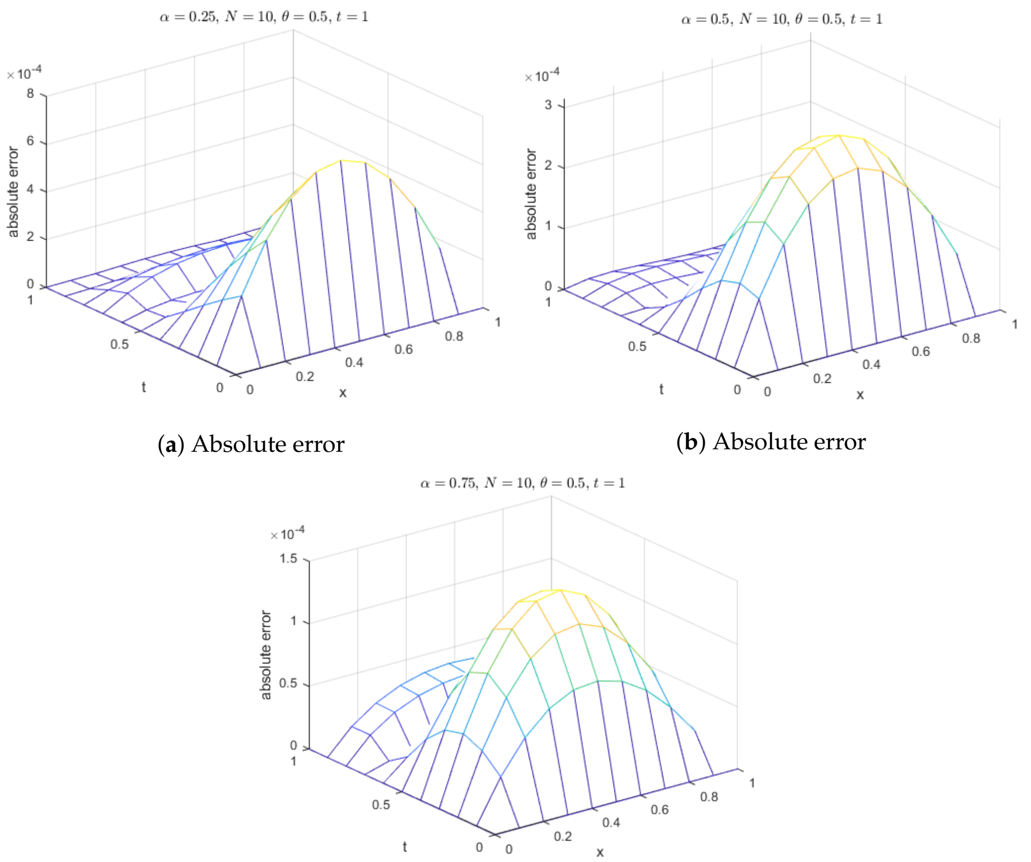

(**a**) Absolute error (**b**) Absolute error

(**c**) Absolute error

Figure 8. Absolute errors for Example 1 with different values of α's using GS RBF.

Example 2. *Let us consider FitzHugh–Nagumo Equations* (2) *and* (3) *with* $\beta = -1$*. The exact solution is given by* [25]

$$u(t,x) = \frac{1}{2} + \frac{1}{2}\tanh\left(\frac{\sqrt{2}x + 3t}{4}\right).$$

The ICs and BCs are derived from the exact solution. The approximate solution is computed using various RBFs such as MQ, IMQ, IQ, and GS with parameters $N = 10$, $\delta t = 0.1$, $\theta = 0.5$, *and* $\alpha = 0.25, 0.5, 0.75, 1$*. The present method is evaluated, and the results are recorded in Tables* 5 *and* 6 *at various node points. These results are then compared with FRDTM. It can be seen that the computed solutions are more accurate than the cited method. All the RBFs exhibit good accuracy even for a small value of* α*.*

Furthermore, for $x \in [0,1]$*, error norms at various time levels are recorded in Tables* 7 *and* 8 *using MQ, IMQ, IQ, and GS RBFs with parameters* $N = 10$, $\delta t = 0.1$, *and* $\theta = 0.5$ *and for different values of* α *(0.25, 0.5, 0.75, and 1). Stability and error norm plots are displayed for MQ, IMQ, IQ, and GS RBFs against the shape parameter in Figure* 9*, which clearly show that the present method fully satisfies the Lax–Richtmyer stability criterion. Surface plots are presented in Figure* 10*, illustrating that the computed solutions using these RBFs closely match the exact solution. Absolute errors for* $\alpha = 1$ *at various time levels are shown in Figure* 11*, indicating reasonable accuracy. Additionally, in Figure* 12*, a comparison between the exact and computed solutions at the final time is displayed, demonstrating the good accuracy of the present method. Finally, Figures* 13*–*16 *present the absolute errors for different RBFs when considering fractional order, highlighting their performance.*

Table 5. Comparison of computed values of the present method solution with FRDTM using MQ, IMQ, IQ, and GS RBFs for $\alpha = 0.25, 0.5$, $\beta = -1$, $N = 10$, $\theta = 0.5$, and $\delta t = 0.1$ corresponds to Example 2.

(x, t)	Exact	$\alpha = 0.25$					$\alpha = 0.5$				
		[25]	MQ	IMQ	IQ	GS	[25]	MQ	IMQ	IQ	GS
			c = 4.4666	**c = 6.03186**	**c = 6.4267**	**c = 0.35958**		**c = 3.92393**	**c = 5.70391**	**c = 5.55183**	**c = 0.19219**
(0.1, 0.2)	0.591631	0.712693	0.593101	0.592493	0.592342	0.590743	0.685107	0.592535	0.592192	0.592074	0.591955
(0.1, 0.4)	0.661662	0.712224	0.663565	0.662685	0.662345	0.659307	0.727258	0.662760	0.662288	0.662272	0.661768
(0.1, 0.6)	0.725261	0.701487	0.727501	0.726615	0.726035	0.723119	0.741707	0.726324	0.725878	0.725984	0.725129
(0.1, 0.8)	0.780864	0.686791	0.782618	0.782556	0.781355	0.780438	0.739056	0.781578	0.781381	0.781398	0.780881
(0.3, 0.2)	0.625306	0.733926	0.628485	0.627149	0.626822	0.623410	0.712225	0.627311	0.626542	0.626279	0.626011
(0.3, 0.4)	0.692564	0.730566	0.696581	0.694651	0.693921	0.687425	0.748766	0.694919	0.693883	0.693797	0.692771
(0.3, 0.6)	0.752526	0.718291	0.757243	0.755312	0.754041	0.747581	0.758657	0.754761	0.753778	0.753975	0.752209
(0.3, 0.8)	0.804102	0.702703	0.807793	0.807757	0.805025	0.802687	0.752244	0.805574	0.805128	0.805201	0.804145
(0.5, 0.2)	0.657811	0.756506	0.661302	0.659809	0.659448	0.655772	0.738240	0.660064	0.659191	0.658895	0.658579
(0.5, 0.4)	0.721829	0.752516	0.726144	0.723992	0.723195	0.716165	0.770276	0.724394	0.723242	0.723087	0.722032
(0.5, 0.6)	0.777914	0.740736	0.782982	0.780841	0.779420	0.772144	0.777298	0.780297	0.779205	0.779384	0.777545
(0.5, 0.8)	0.825426	0.726144	0.829396	0.829500	0.826306	0.823317	0.769236	0.826965	0.826464	0.826587	0.825521
(0.7, 0.2)	0.688899	0.780077	0.691594	0.690419	0.690140	0.687381	0.763050	0.690677	0.689980	0.689747	0.689481
(0.7, 0.4)	0.749317	0.777418	0.752584	0.750893	0.750280	0.744958	0.791672	0.751279	0.750382	0.750211	0.749455
(0.7, 0.6)	0.801385	0.767864	0.805234	0.803562	0.802439	0.796670	0.797388	0.803170	0.802322	0.802430	0.801100
(0.7, 0.8)	0.844877	0.755857	0.847904	0.848125	0.845470	0.842806	0.789575	0.846004	0.845618	0.845751	0.845024
(0.9, 0.2)	0.718371	0.804119	0.719430	0.718959	0.718850	0.717810	0.786549	0.719084	0.718802	0.718709	0.718593
(0.9, 0.4)	0.774936	0.804312	0.776199	0.775521	0.775281	0.773242	0.812740	0.775698	0.775344	0.775256	0.774984
(0.9, 0.6)	0.822940	0.798295	0.824438	0.823772	0.823318	0.820985	0.818467	0.823620	0.823287	0.823318	0.822838
(0.9, 0.8)	0.862522	0.790062	0.863707	0.863865	0.862729	0.861527	0.812450	0.862941	0.862794	0.862864	0.862627

Table 6. Comparison of computed values of the present method solution with FRDTM using MQ, IMQ, IQ, and GS RBFs for $\alpha = 0.75, 1$, $\beta = -1$, $N = 10$, $\theta = 0.5$, and $\delta t = 0.1$ corresponds to Example 2.

(x, t)	Exact	$\alpha = 0.75$					$\alpha = 1$				
		[25]	MQ	IMQ	IQ	GS	[25]	MQ	IMQ	IQ	GS
			c = 4.80554	**c = 5.17758**	**c = 5.90952**	**c = 0.20069**		**c = 6.47961**	**c = 5.51787**	**c = 6.45128**	**c = 0.19927**
(0.1, 0.2)	0.591631	0.634779	0.591992	0.591864	0.591837	0.591767	0.591631	0.591628	0.591633	0.591632	0.591620
(0.1, 0.4)	0.661662	0.702543	0.662181	0.661959	0.661901	0.661733	0.661672	0.661649	0.661667	0.661662	0.661628
(0.1, 0.6)	0.725261	0.747913	0.725872	0.725535	0.725459	0.725237	0.725403	0.725246	0.725272	0.725258	0.725197
(0.1, 0.8)	0.780864	0.774078	0.781331	0.781026	0.781074	0.780806	0.781773	0.780862	0.780876	0.780859	0.780768
(0.3, 0.2)	0.625306	0.666335	0.626111	0.625833	0.625768	0.625606	0.625306	0.625302	0.625314	0.625312	0.625284
(0.3, 0.4)	0.692564	0.729310	0.693682	0.693228	0.693080	0.692711	0.692582	0.692538	0.692581	0.692572	0.692491
(0.3, 0.6)	0.752526	0.769312	0.753809	0.753125	0.752937	0.752464	0.752748	0.752494	0.752557	0.752531	0.752396
(0.3, 0.8)	0.804102	0.789838	0.805115	0.804456	0.804526	0.803957	0.805411	0.804095	0.804133	0.804104	0.803895
(0.5, 0.2)	0.657811	0.696497	0.658719	0.658414	0.658337	0.658141	0.657811	0.657808	0.657823	0.657821	0.657786
(0.5, 0.4)	0.721829	0.754683	0.723053	0.722590	0.722397	0.721980	0.721853	0.721803	0.721858	0.721849	0.721749
(0.5, 0.6)	0.777914	0.789950	0.779284	0.778586	0.778350	0.777837	0.778188	0.777881	0.777959	0.777936	0.777778
(0.5, 0.8)	0.825426	0.806094	0.826535	0.825827	0.825872	0.825257	0.826971	0.825416	0.825467	0.825446	0.825201
(0.7, 0.2)	0.688899	0.725094	0.689618	0.689385	0.689319	0.689149	0.688899	0.688896	0.688911	0.688910	0.688877
(0.7, 0.4)	0.749317	0.778610	0.750257	0.749934	0.749755	0.749423	0.749343	0.749298	0.749349	0.749342	0.749253
(0.7, 0.6)	0.801385	0.809841	0.802413	0.801920	0.801715	0.801324	0.801677	0.801361	0.801430	0.801416	0.801284
(0.7, 0.8)	0.844877	0.822859	0.845727	0.845204	0.845215	0.844750	0.846479	0.844868	0.844914	0.844909	0.844705
(0.9, 0.2)	0.718371	0.751995	0.718660	0.718571	0.718542	0.718465	0.718372	0.718370	0.718378	0.718377	0.718361
(0.9, 0.4)	0.774936	0.801046	0.775302	0.775193	0.775108	0.774973	0.774962	0.774928	0.774953	0.774950	0.774909
(0.9, 0.6)	0.822940	0.828936	0.823333	0.823160	0.823070	0.822918	0.823220	0.822932	0.822962	0.822959	0.822902
(0.9, 0.8)	0.862522	0.839976	0.862853	0.862662	0.862657	0.862479	0.864017	0.862518	0.862539	0.862542	0.862455

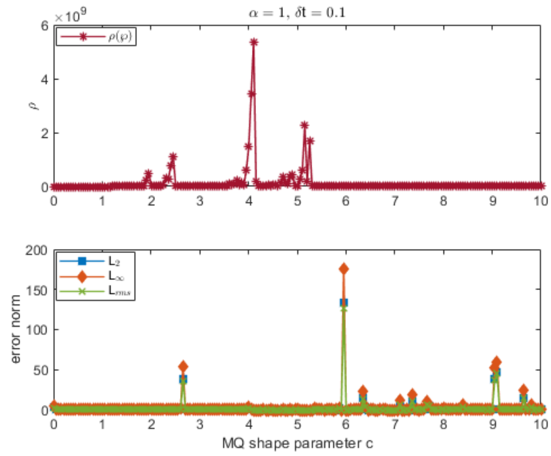

(**a**) Error norms and spectral radius using MQ

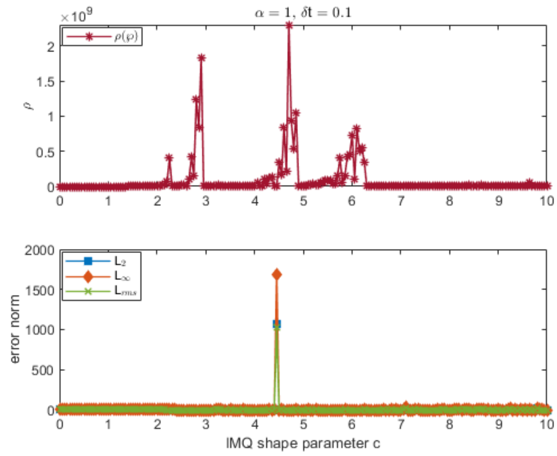

(**b**) Error norms and spectral radius using IMQ

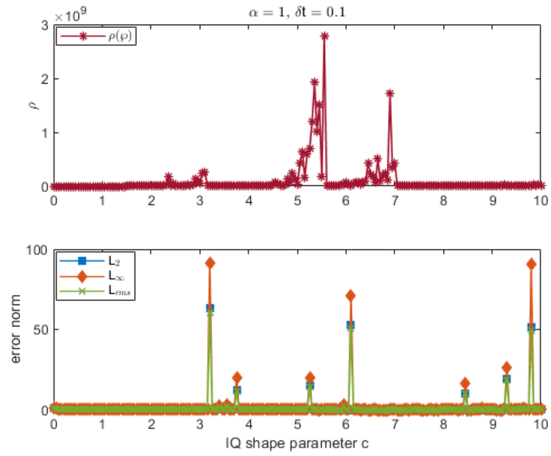

(**c**) Error norms and spectral radius against IQ

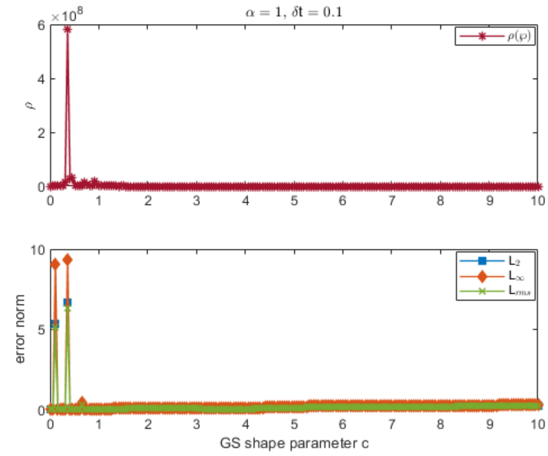

(**d**) Error norms and spectral radius using GS

Figure 9. Error norms and spectral radius correspond to Example 2 when N = M = 10, $\theta = 0.5$ using MQ, IMQ, IQ, and GS RBFs.

Table 7. Error norms at various time levels using MQ, IMQ, IQ, and GS RBFs for $\alpha = 0.25, 0.5$, $\beta = -1$, N = 10, $\theta = 0.5$, and $\delta t = 0.1$ correspond to Example 2.

RBFs	**t**	$\alpha = 0.25$			$\alpha = 0.5$		
		L_2	L_∞	L_{rms}	L_2	L_∞	L_{rms}
MQ		c = 4.4666			c = 3.92393		
	0.2	2.56×10^{-3}	3.49×10^{-3}	2.44×10^{-3}	1.65×10^{-3}	2.25×10^{-3}	1.57×10^{-3}
	0.4	3.18×10^{-3}	4.36×10^{-3}	3.03×10^{-3}	1.88×10^{-3}	2.58×10^{-3}	1.80×10^{-3}
	0.6	3.74×10^{-3}	5.12×10^{-3}	3.56×10^{-3}	1.76×10^{-3}	2.42×10^{-3}	1.67×10^{-3}
	0.8	2.93×10^{-3}	4.01×10^{-3}	2.79×10^{-3}	1.14×10^{-3}	1.58×10^{-3}	1.09×10^{-3}
	1	3.66×10^{-5}	5.14×10^{-5}	3.49×10^{-5}	3.49×10^{-6}	5.48×10^{-6}	3.32×10^{-6}
IMQ		c = 6.03186			c = 5.70391		
	0.2	1.47×10^{-3}	2.01×10^{-3}	1.40×10^{-3}	1.01×10^{-3}	1.38×10^{-3}	9.63×10^{-4}
	0.4	1.61×10^{-3}	2.23×10^{-3}	1.53×10^{-3}	1.04×10^{-3}	1.43×10^{-3}	9.93×10^{-4}
	0.6	2.17×10^{-3}	2.99×10^{-3}	2.07×10^{-3}	9.59×10^{-4}	1.33×10^{-3}	9.14×10^{-4}
	0.8	3.00×10^{-3}	4.07×10^{-3}	2.86×10^{-3}	7.76×10^{-4}	1.08×10^{-3}	7.40×10^{-4}
	1	1.08×10^{-5}	1.83×10^{-5}	1.03×10^{-5}	5.36×10^{-6}	8.29×10^{-6}	5.11×10^{-6}

Table 7. *Cont.*

RBFs	t	$\alpha = 0.25$			$\alpha = 0.5$		
		L_2	L_∞	L_{rms}	L_2	L_∞	L_{rms}
IQ			c = 6.4267			c = 5.55183	
	0.2	1.20×10^{-3}	1.65×10^{-3}	1.15×10^{-3}	7.93×10^{-4}	1.08×10^{-3}	7.56×10^{-4}
	0.4	1.02×10^{-3}	1.43×10^{-3}	9.73×10^{-4}	9.34×10^{-4}	1.31×10^{-3}	8.91×10^{-4}
	0.6	1.13×10^{-3}	1.58×10^{-3}	1.08×10^{-3}	1.10×10^{-3}	1.53×10^{-3}	1.04×10^{-3}
	0.8	6.71×10^{-4}	9.45×10^{-4}	6.40×10^{-4}	8.61×10^{-4}	1.18×10^{-3}	8.21×10^{-4}
	1	1.45×10^{-5}	2.48×10^{-5}	1.38×10^{-5}	6.97×10^{-6}	1.10×10^{-5}	6.64×10^{-6}
GS			c = 0.35958			c = 0.19219	
	0.2	1.49×10^{-3}	2.06×10^{-3}	1.42×10^{-3}	5.62×10^{-4}	7.72×10^{-4}	5.36×10^{-4}
	0.4	4.14×10^{-3}	5.66×10^{-3}	3.95×10^{-3}	1.53×10^{-4}	2.16×10^{-4}	1.45×10^{-4}
	0.6	4.20×10^{-3}	5.77×10^{-3}	4.01×10^{-3}	2.63×10^{-4}	3.69×10^{-4}	2.51×10^{-4}
	0.8	1.54×10^{-3}	2.20×10^{-3}	1.47×10^{-3}	9.23×10^{-5}	1.46×10^{-4}	8.80×10^{-5}
	1	3.07×10^{-5}	5.19×10^{-5}	2.93×10^{-5}	1.25×10^{-5}	2.32×10^{-5}	1.19×10^{-5}

Table 8. Error norms at various time levels using MQ, IMQ, IQ, and GS RBFs for $\alpha = 0.75, 1$, $\beta = -1$, N = 10, $\theta = 0.5$, and $\delta t = 0.1$ correspond to Example 2.

RBFs	t	$\alpha = 0.75$			$\alpha = 1$		
		L_2	L_∞	L_{rms}	L_2	L_∞	L_{rms}
MQ			c = 4.80554			c = 6.47961	
	0.2	6.64×10^{-4}	9.08×10^{-4}	6.33×10^{-4}	2.74×10^{-6}	3.70×10^{-6}	2.61×10^{-6}
	0.4	8.97×10^{-4}	1.23×10^{-3}	8.56×10^{-4}	2.01×10^{-5}	2.76×10^{-5}	1.91×10^{-5}
	0.6	1.01×10^{-3}	1.39×10^{-3}	9.63×10^{-4}	2.46×10^{-5}	3.44×10^{-5}	2.35×10^{-5}
	0.8	8.12×10^{-4}	1.11×10^{-3}	7.74×10^{-4}	7.31×10^{-6}	1.02×10^{-5}	6.97×10^{-6}
	1	4.55×10^{-6}	7.31×10^{-6}	4.34×10^{-6}	5.95×10^{-7}	8.99×10^{-7}	5.67×10^{-7}
IMQ			c = 5.17758			c = 5.51787	
	0.2	4.41×10^{-4}	6.04×10^{-4}	4.20×10^{-4}	8.95×10^{-6}	1.28×10^{-5}	8.54×10^{-6}
	0.4	5.57×10^{-4}	7.60×10^{-4}	5.31×10^{-4}	2.21×10^{-5}	3.19×10^{-5}	2.10×10^{-5}
	0.6	4.93×10^{-4}	6.71×10^{-4}	4.70×10^{-4}	3.31×10^{-5}	4.66×10^{-5}	3.16×10^{-5}
	0.8	2.96×10^{-4}	4.01×10^{-4}	2.82×10^{-4}	2.96×10^{-5}	4.07×10^{-5}	2.82×10^{-5}
	1	1.30×10^{-6}	2.26×10^{-6}	1.24×10^{-6}	5.23×10^{-7}	8.30×10^{-7}	4.99×10^{-7}
IQ			c = 5.90952			c = 6.45128	
	0.2	3.84×10^{-4}	5.26×10^{-4}	3.66×10^{-4}	7.91×10^{-6}	1.14×10^{-5}	7.54×10^{-6}
	0.4	4.16×10^{-4}	5.68×10^{-4}	3.97×10^{-4}	1.58×10^{-5}	2.46×10^{-5}	1.51×10^{-5}
	0.6	3.23×10^{-4}	4.43×10^{-4}	3.08×10^{-4}	1.87×10^{-5}	3.05×10^{-5}	1.78×10^{-5}
	0.8	3.33×10^{-4}	4.54×10^{-4}	3.17×10^{-4}	1.88×10^{-5}	3.13×10^{-5}	1.80×10^{-5}
	1	1.29×10^{-6}	1.89×10^{-6}	1.23×10^{-6}	1.05×10^{-6}	1.81×10^{-6}	1.00×10^{-6}
GS			c = 0.20069			c = 0.19927	
	0.2	2.40×10^{-4}	3.31×10^{-4}	2.29×10^{-4}	1.90×10^{-5}	2.50×10^{-5}	1.81×10^{-5}
	0.4	1.11×10^{-4}	1.57×10^{-4}	1.06×10^{-4}	5.96×10^{-5}	8.05×10^{-5}	5.69×10^{-5}
	0.6	5.43×10^{-5}	7.71×10^{-5}	5.18×10^{-5}	1.02×10^{-4}	1.40×10^{-4}	9.67×10^{-5}
	0.8	1.19×10^{-4}	1.69×10^{-4}	1.14×10^{-4}	1.65×10^{-4}	2.26×10^{-4}	1.58×10^{-4}
	1	9.36×10^{-6}	1.59×10^{-5}	8.93×10^{-6}	5.69×10^{-6}	8.86×10^{-6}	5.43×10^{-6}

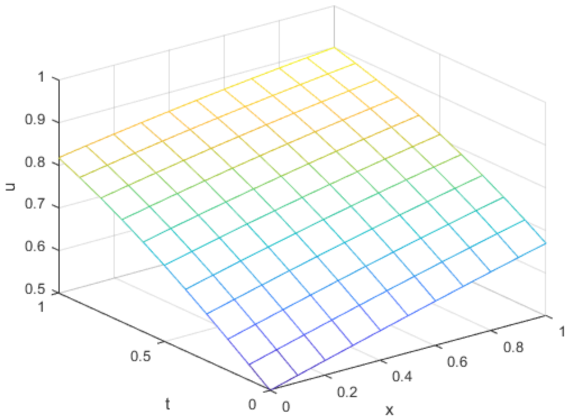

(**a**) Exact solution

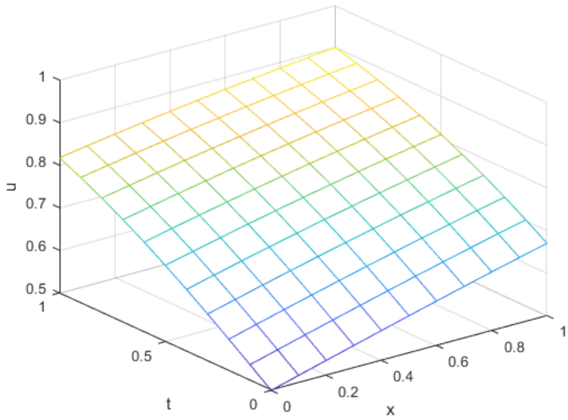

(**b**) Computed solution using MQ

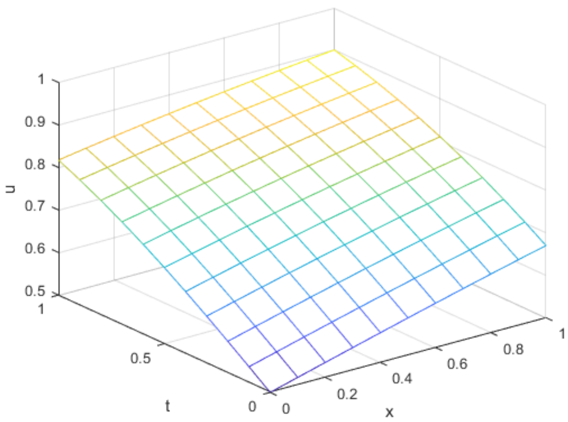

(**c**) Computed solution using IMQ

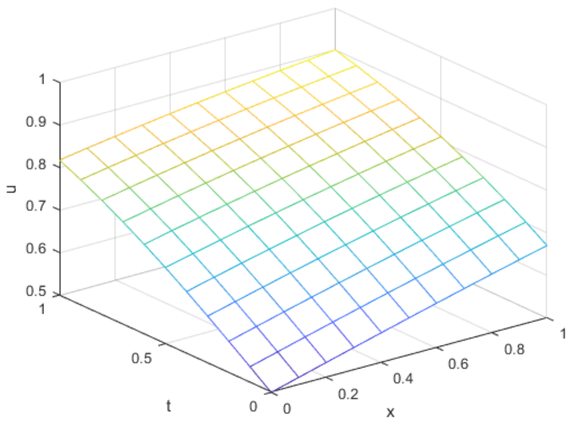

(**d**) Computed solution against IQ

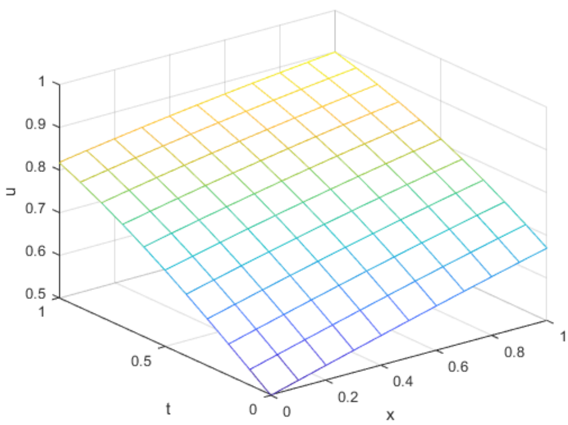

(**e**) Computed solution using GS

Figure 10. Exact vs. computed solution corresponds to Example 2 when $N = M = 10$, $\alpha = 1$ using MQ, IMQ, IQ, and GS RBFs.

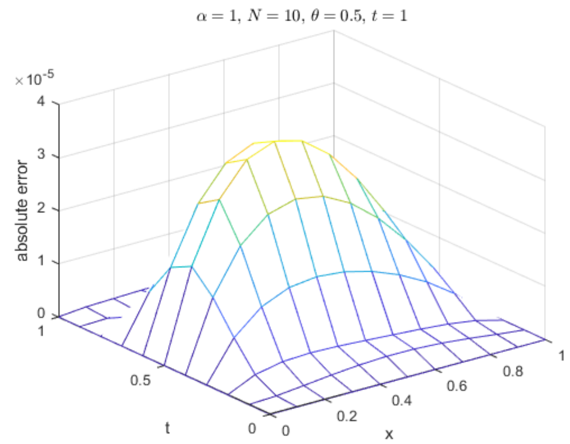

(**a**) Absolute error using MQ

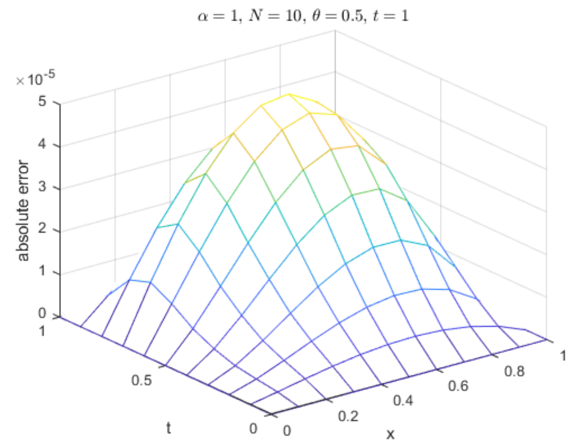

(**b**) Absolute error using IMQ

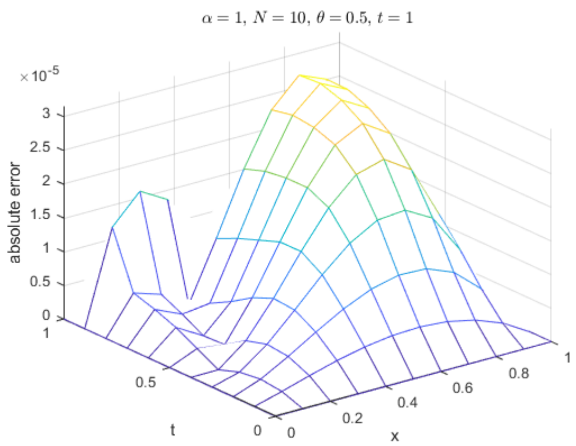

(**c**) Absolute error against IQ

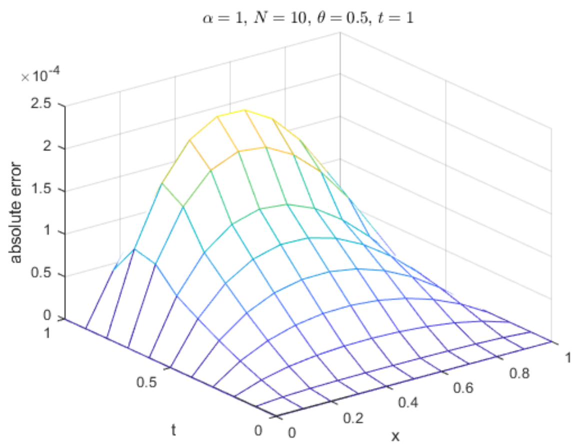

(**d**) Absolute error using GS

Figure 11. Absolute error of MQ, IMQ, IQ, and GS at $t_{max} = 1$ corresponds to Example 2.

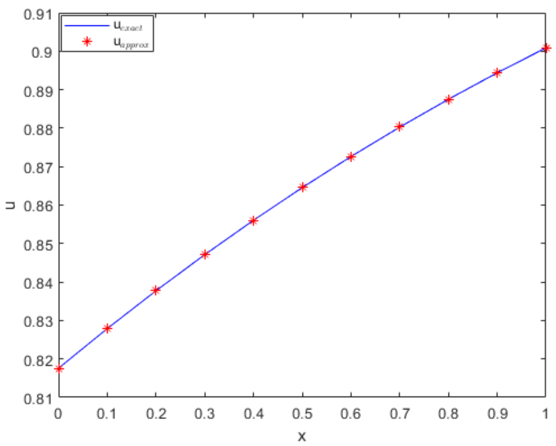

(**a**) Exact vs. numerical using MQ

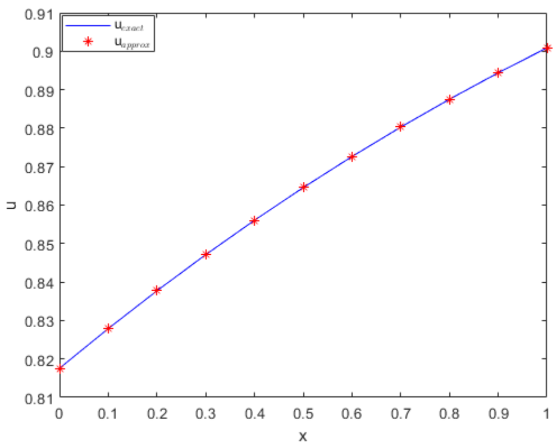

(**b**) Exact vs. numerical using IMQ

Figure 12. *Cont*.

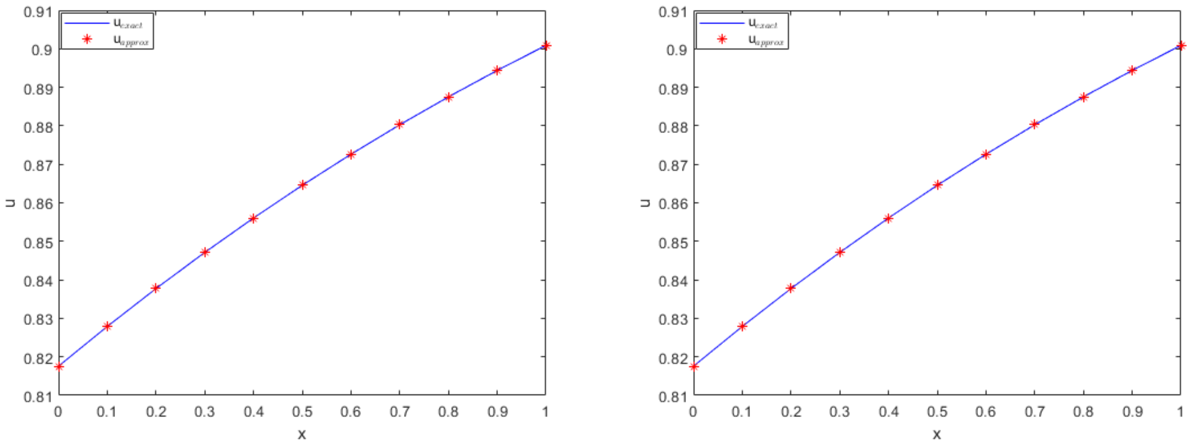

(**c**) Exact vs. numerical against IQ (**d**) Exact vs. numerical using GS

Figure 12. Comparison of exact and computed solution corresponds to Example 2 at $t_{max} = 1$ and $\alpha = 1$ using MQ, IMQ, IQ, and GS RBFs.

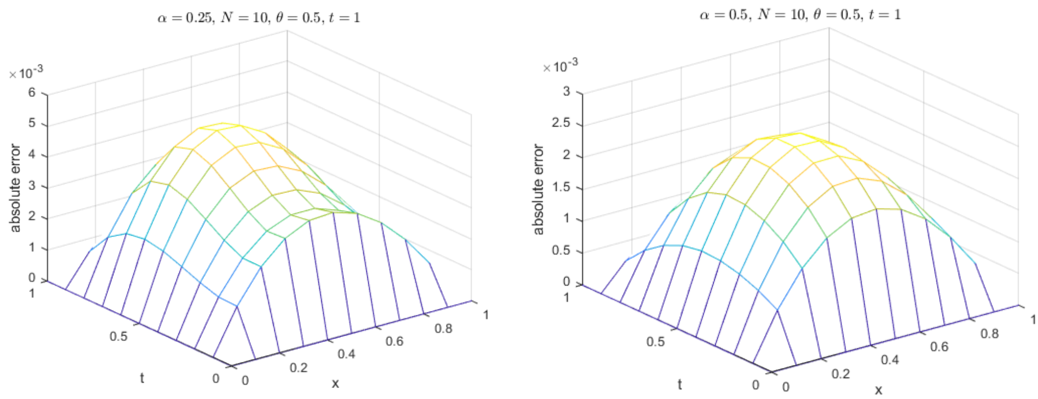

(**a**) Absolute error (**b**) Absolute error

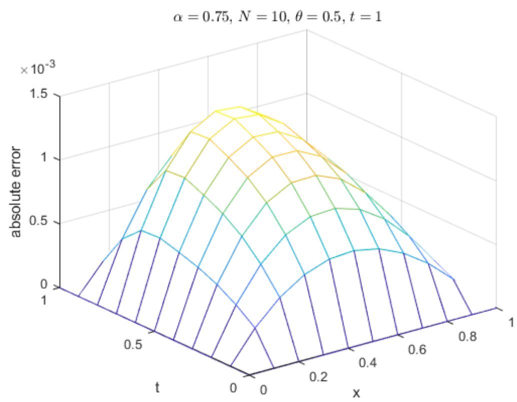

(**c**) Absolute error

Figure 13. Absolute errors for Example 3 with different values of α's using MQ RBF.

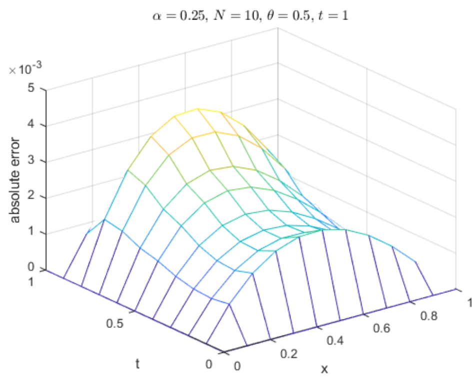

(**a**) Absolute error

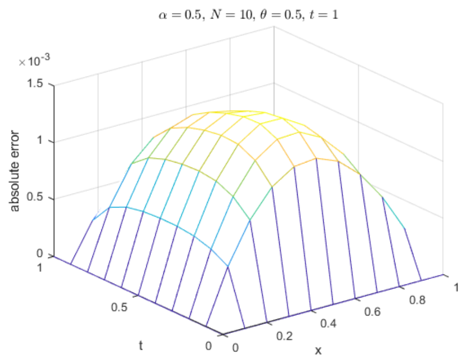

(**b**) Absolute error

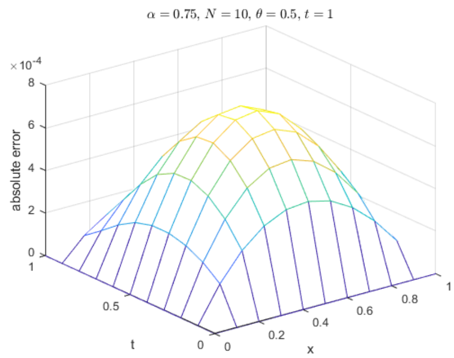

(**c**) Absolute error

Figure 14. Absolute errors for Example 3 with different values of α's using IMQ RBF.

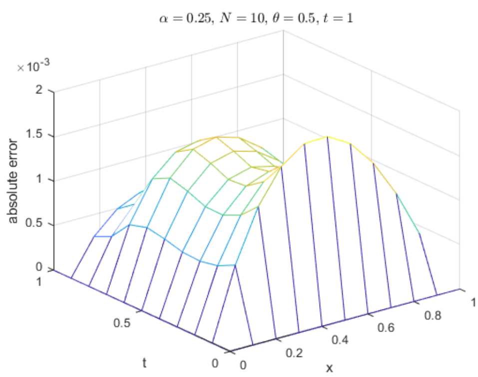

(**a**) Absolute error

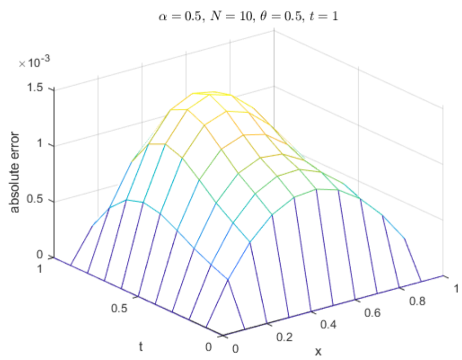

(**b**) Absolute error

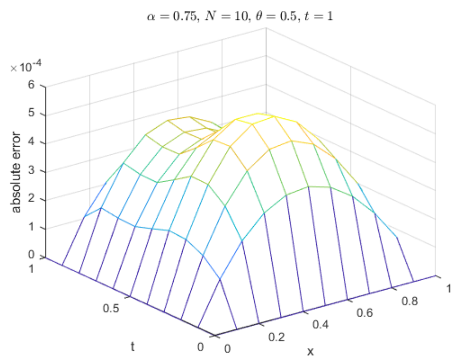

(**c**) Absolute error

Figure 15. Absolute errors for Example 3 with different values of α's using IQ RBF.

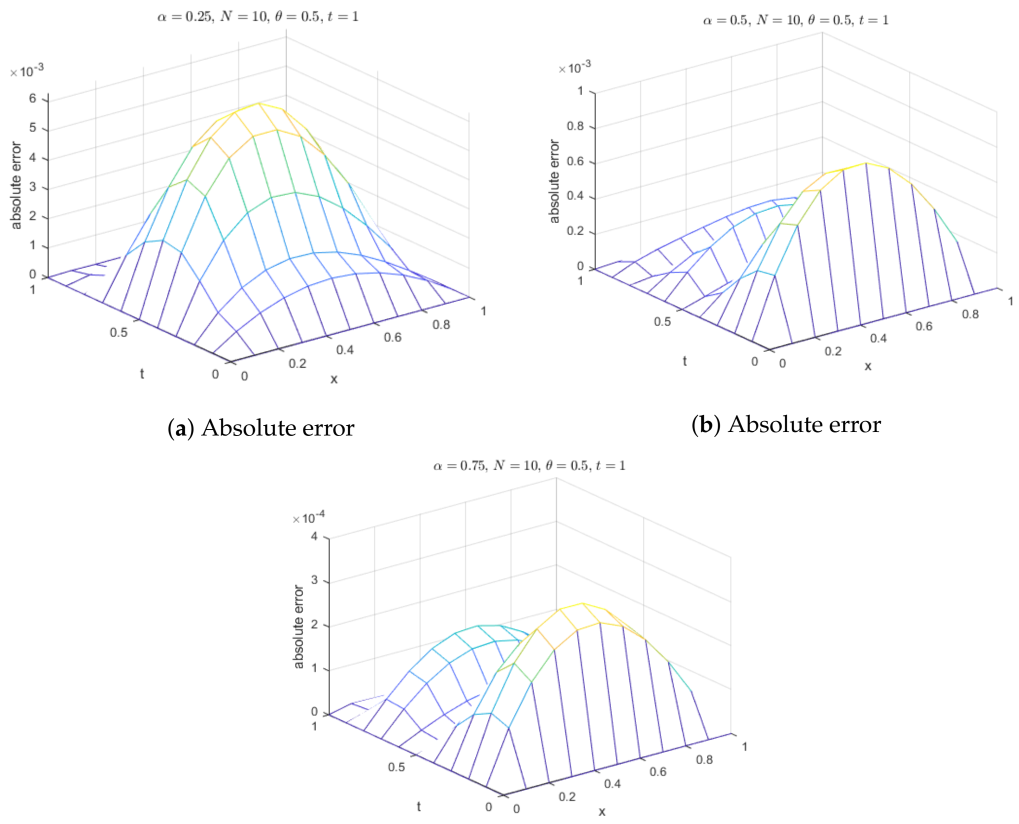

(**a**) Absolute error (**b**) Absolute error

(**c**) Absolute error

Figure 16. Absolute errors for Example 3 with different values of α's using GS RBF.

Example 3. *Let us consider FitzHugh–Nagumo Equations* (2) *and* (3) *with* $\beta = 0$*. The exact solution is given by [25]*

$$u(t,x) = \frac{1}{2} + \frac{1}{2}\tanh\left(\frac{\sqrt{2}x + t}{4}\right).$$

We employ the ICs and BCs from this exact solution. Using this solution, we apply the present method to approximate the exact solution within the domain $x \in [0,1]$*. RBFs such as MQ, IMQ, IQ, and GS are employed for the numerical approximation. We choose* $N = 10$, $\delta t = 0.1$*, and* $\theta = 0.5$*. The obtained results are presented in Tables 9 and 10 for different values of* α $(0.25, 0.5, 0.75, 1)$*.*

The tables clearly indicate that the accuracy of the method is better than the FRDTM. Additionally, it can be seen that the accuracy improves as α *approaches 1. Additionally, the chosen RBFs demonstrate comparable performance. Furthermore, the error norms at various time levels are recorded in Tables 11 and 12 for* α *values of* 0.25, 0.5, 0.75, *and* 1*, using the MQ, IMQ, IQ, and GS RBFs. The stability and error norm plots are presented in Figure 17, demonstrating that the present method consistently satisfies the Lax–Richtmyer stability criterion.*

Additionally, surface plots in Figure 18 show that the computed solution using the selected RBFs closely matches the exact solution. The absolute errors for $\alpha = 1$ *at various time levels are depicted in Figure 19, indicating reasonable accuracy. Figure 20 compares the exact and computed solutions at the final time, demonstrating the good accuracy of the present method. Finally, Figures 21–24 display the absolute errors for different fractional orders using different RBFs.*

Table 9. Comparison of computed values of the present method solution with FRDTM using MQ, IMQ, IQ, and GS RBFs for $\alpha = 0.25, 0.5$, $\beta = 0$, $\mathrm{N} = 10$, $\theta = 0.5$, and $\delta\mathrm{t} = 0.1$ corresponds to Example 3.

(x, t)	Exact	$\alpha = 0.25$					$\alpha = 0.5$				
		[25]	MQ c = 3.68162	IMQ c = 6.61203	IQ c = 8.81199	GS c = 0.36854	[25]	MQ c = 6.48549	IMQ c = 7.63322	IQ c = 6.9269	GS c = 0.33014
(0.1, 0.2)	0.542574	0.607541	0.543147	0.543015	0.542936	0.542301	0.579728	0.542826	0.542838	0.542813	0.542595
(0.1, 0.4)	0.567267	0.624171	0.567777	0.567728	0.567539	0.566309	0.604611	0.567451	0.567615	0.567554	0.567328
(0.1, 0.6)	0.591631	0.635373	0.592090	0.592066	0.591836	0.590916	0.623334	0.591672	0.591984	0.591826	0.591753
(0.1, 0.8)	0.615552	0.644106	0.615894	0.615880	0.615667	0.615606	0.638889	0.615523	0.615760	0.615571	0.615607
(0.3, 0.2)	0.577406	0.639862	0.578702	0.578408	0.578231	0.576967	0.613492	0.577980	0.578005	0.577953	0.577472
(0.3, 0.4)	0.601599	0.655466	0.602729	0.602641	0.602231	0.599800	0.637390	0.602020	0.602392	0.602265	0.601792
(0.3, 0.6)	0.625306	0.665857	0.626309	0.626280	0.625790	0.623770	0.655204	0.625410	0.626117	0.625769	0.625657
(0.3, 0.8)	0.648427	0.673883	0.649148	0.649157	0.648699	0.648556	0.669886	0.648373	0.648923	0.648480	0.648661
(0.5, 0.2)	0.611484	0.670946	0.612968	0.612638	0.612435	0.611202	0.646202	0.612144	0.612174	0.612119	0.611584
(0.5, 0.4)	0.634960	0.685416	0.636223	0.636155	0.635702	0.633346	0.668940	0.635440	0.635874	0.635739	0.635255
(0.5, 0.6)	0.657811	0.694923	0.658913	0.658914	0.658388	0.656165	0.685729	0.657930	0.658750	0.658358	0.658312
(0.5, 0.8)	0.679952	0.702183	0.680713	0.680772	0.680279	0.680129	0.699451	0.679896	0.680535	0.680019	0.680357
(0.7, 0.2)	0.644506	0.700614	0.645694	0.645439	0.645271	0.644477	0.677605	0.645032	0.645063	0.645023	0.644609
(0.7, 0.4)	0.667073	0.713905	0.668059	0.668036	0.667684	0.666161	0.699052	0.667449	0.667813	0.667710	0.667379
(0.7, 0.6)	0.688899	0.722509	0.689742	0.689775	0.689383	0.687690	0.714740	0.688986	0.689660	0.689347	0.689393
(0.7, 0.8)	0.709916	0.728997	0.710468	0.710559	0.710191	0.710100	0.727453	0.709870	0.710385	0.709969	0.710363
(0.9, 0.2)	0.676207	0.728724	0.676688	0.676590	0.676519	0.676287	0.707489	0.676418	0.676435	0.676422	0.676262
(0.9, 0.4)	0.697706	0.740845	0.698094	0.698100	0.697961	0.697504	0.727556	0.697851	0.698010	0.697969	0.697863
(0.9, 0.6)	0.718371	0.748576	0.718695	0.718725	0.718578	0.717935	0.742105	0.718399	0.718684	0.718556	0.718617
(0.9, 0.8)	0.738154	0.754327	0.738351	0.738410	0.738273	0.738255	0.753800	0.738134	0.738342	0.738175	0.738393

Table 10. Comparison of computed values of the present method solution with FRDTM using MQ, IMQ, IQ, and GS RBFs for $\alpha = 0.75, 1$, $\beta = 0$, $\mathrm{N} = 10$, $\theta = 0.5$, and $\delta\mathrm{t} = 0.1$ corresponds to Example 3.

(x, t)	Exact	$\alpha = 0.75$					$\alpha = 1$				
		[25]	MQ c = 6.20135	IMQ c = 7.82578	IQ c = 6.73987	GS c = 0.333513	[25]	MQ c = 5.79129	IMQ c = 6.46003	IQ c = 8.05516	GS c = 0.22009
(0.1, 0.2)	0.542574	0.558029	0.542671	0.542661	0.542670	0.542575	0.542574	0.542576	0.542575	0.542570	0.542596
(0.1, 0.4)	0.567267	0.585031	0.567267	0.567359	0.567431	0.567193	0.567267	0.567272	0.567265	0.567252	0.567332
(0.1, 0.6)	0.591631	0.608198	0.591550	0.591683	0.591797	0.591527	0.591626	0.591638	0.591632	0.591658	0.591702
(0.1, 0.8)	0.615552	0.628969	0.615483	0.615541	0.615611	0.615522	0.615532	0.615559	0.615549	0.615646	0.615591
(0.3, 0.2)	0.577406	0.592512	0.577628	0.577605	0.577625	0.577403	0.577406	0.577409	0.577407	0.577397	0.577451
(0.3, 0.4)	0.601599	0.618758	0.601608	0.601811	0.601981	0.601363	0.601598	0.601610	0.601598	0.601567	0.601745
(0.3, 0.6)	0.625306	0.641090	0.625128	0.625431	0.625694	0.624963	0.625302	0.625322	0.625313	0.625358	0.625473
(0.3, 0.8)	0.648427	0.660973	0.648272	0.648398	0.648570	0.648301	0.648409	0.648443	0.648426	0.648650	0.648523
(0.5, 0.2)	0.611484	0.626109	0.611740	0.611714	0.611741	0.611473	0.611484	0.611487	0.611487	0.611475	0.611535
(0.5, 0.4)	0.634960	0.651378	0.634968	0.635204	0.635411	0.634600	0.634959	0.634972	0.634963	0.634927	0.635130
(0.5, 0.6)	0.657811	0.672710	0.657602	0.657954	0.658267	0.657287	0.657807	0.657830	0.657824	0.657873	0.658009
(0.5, 0.8)	0.679952	0.691573	0.679774	0.679907	0.680117	0.679745	0.679938	0.679971	0.679957	0.680214	0.680069
(0.7, 0.2)	0.644506	0.658533	0.644709	0.644690	0.644717	0.644489	0.644506	0.644509	0.644509	0.644499	0.644550
(0.7, 0.4)	0.667073	0.682643	0.667064	0.667266	0.667449	0.666697	0.667072	0.667083	0.667079	0.667048	0.667216
(0.7, 0.6)	0.688899	0.702841	0.688718	0.689008	0.689272	0.688366	0.688896	0.688914	0.688914	0.688963	0.689063
(0.7, 0.8)	0.709916	0.720587	0.709770	0.709863	0.710039	0.709701	0.709906	0.709931	0.709924	0.710127	0.710012
(0.9, 0.2)	0.676207	0.689541	0.676288	0.676281	0.676296	0.676195	0.676207	0.676209	0.676209	0.676204	0.676228
(0.9, 0.4)	0.697706	0.712345	0.697691	0.697781	0.697866	0.697510	0.697705	0.697710	0.697710	0.697697	0.697768
(0.9, 0.6)	0.718371	0.731313	0.718289	0.718410	0.718525	0.718106	0.718370	0.718378	0.718380	0.718410	0.718440
(0.9, 0.8)	0.738154	0.747877	0.738093	0.738123	0.738198	0.738049	0.738149	0.738160	0.738160	0.738238	0.738194

Table 11. Error norms at various time levels using MQ, IMQ, IQ, and GS RBFs for $\alpha = 0.25, 0.5$, $\beta = 0$, $N = 10$, $\theta = 0.5$, and $\delta t = 0.1$ correspond to Example 3.

RBFs	t	$\alpha = 0.25$			$\alpha = 0.5$		
		L_2	L_∞	L_{rms}	L_2	L_∞	L_{rms}
MQ		c = 3.68162			c = 6.48549		
	0.2	1.081×10^{-3}	1.484×10^{-3}	1.031×10^{-3}	4.795×10^{-4}	6.599×10^{-4}	4.572×10^{-4}
	0.4	9.220×10^{-4}	1.264×10^{-3}	8.791×10^{-4}	3.476×10^{-4}	4.805×10^{-4}	3.314×10^{-4}
	0.6	8.053×10^{-4}	1.103×10^{-3}	7.678×10^{-4}	8.368×10^{-5}	1.193×10^{-4}	7.978×10^{-5}
	0.8	5.578×10^{-4}	7.776×10^{-4}	5.319×10^{-4}	4.336×10^{-5}	5.738×10^{-5}	4.134×10^{-5}
	1	2.992×10^{-6}	4.995×10^{-6}	2.853×10^{-6}	2.723×10^{-6}	3.734×10^{-6}	2.597×10^{-6}
IMQ		c = 6.61203			c = 7.63322		
	0.2	8.418×10^{-4}	1.154×10^{-3}	8.027×10^{-4}	5.035×10^{-4}	6.907×10^{-4}	4.801×10^{-4}
	0.4	8.722×10^{-4}	1.195×10^{-3}	8.316×10^{-4}	6.669×10^{-4}	9.148×10^{-4}	6.358×10^{-4}
	0.6	8.053×10^{-4}	1.103×10^{-3}	7.679×10^{-4}	6.838×10^{-4}	9.390×10^{-4}	6.519×10^{-4}
	0.8	5.980×10^{-4}	8.194×10^{-4}	5.702×10^{-4}	4.202×10^{-4}	5.823×10^{-4}	4.007×10^{-4}
	1	1.530×10^{-6}	2.163×10^{-6}	1.458×10^{-6}	3.049×10^{-6}	5.391×10^{-6}	2.907×10^{-6}
IQ		c = 8.81199			c = 6.9269		
	0.2	6.924×10^{-4}	9.508×10^{-4}	6.602×10^{-4}	4.630×10^{-4}	6.348×10^{-4}	4.414×10^{-4}
	0.4	5.406×10^{-4}	7.424×10^{-4}	5.154×10^{-4}	5.671×10^{-4}	7.799×10^{-4}	5.407×10^{-4}
	0.6	4.209×10^{-4}	5.776×10^{-4}	4.013×10^{-4}	3.965×10^{-4}	5.470×10^{-4}	3.780×10^{-4}
	0.8	2.383×10^{-4}	3.268×10^{-4}	2.272×10^{-4}	4.684×10^{-5}	6.663×10^{-5}	4.466×10^{-5}
	1	7.249×10^{-7}	1.173×10^{-6}	6.912×10^{-7}	2.578×10^{-6}	3.610×10^{-6}	2.458×10^{-6}
GS		c = 0.36854			c = 0.33014		
	0.2	2.642×10^{-4}	4.388×10^{-4}	2.519×10^{-4}	7.528×10^{-5}	1.068×10^{-4}	7.178×10^{-5}
	0.4	1.233×10^{-3}	1.803×10^{-3}	1.175×10^{-3}	2.218×10^{-4}	3.161×10^{-4}	2.115×10^{-4}
	0.6	1.202×10^{-3}	1.671×10^{-3}	1.146×10^{-3}	3.722×10^{-4}	5.227×10^{-4}	3.549×10^{-4}
	0.8	1.376×10^{-4}	1.881×10^{-4}	1.312×10^{-4}	3.090×10^{-4}	4.497×10^{-4}	2.946×10^{-4}
	1	9.904×10^{-6}	1.513×10^{-5}	9.443×10^{-6}	6.429×10^{-6}	1.094×10^{-5}	6.130×10^{-6}

Table 12. Error norms at various time levels using MQ, IMQ, IQ, and GS RBFs for $\alpha = 0.75, 1$, $\beta = 0$, $N = 10$, $\theta = 0.5$, and $\delta t = 0.1$ correspond to Example 3.

RBFs	t	$\alpha = 0.75$			$\alpha = 1$		
		L_2	L_∞	L_{rms}	L_2	L_∞	L_{rms}
MQ		c = 6.20135			c = 5.79129		
	0.2	1.854×10^{-4}	2.561×10^{-4}	1.768×10^{-4}	2.754×10^{-6}	3.671×10^{-6}	2.626×10^{-6}
	0.4	9.181×10^{-6}	1.560×10^{-5}	8.754×10^{-6}	9.160×10^{-6}	1.245×10^{-5}	8.734×10^{-6}
	0.6	1.553×10^{-4}	2.091×10^{-4}	1.481×10^{-4}	1.392×10^{-5}	1.900×10^{-5}	1.327×10^{-5}
	0.8	1.306×10^{-4}	1.781×10^{-4}	1.245×10^{-4}	1.335×10^{-5}	1.841×10^{-5}	1.273×10^{-5}
	1	1.342×10^{-6}	2.211×10^{-6}	1.280×10^{-6}	4.507×10^{-7}	7.729×10^{-7}	4.298×10^{-7}
IMQ		c = 7.82578			c = 6.46003		
	0.2	1.672×10^{-4}	2.305×10^{-4}	1.594×10^{-4}	2.380×10^{-6}	3.590×10^{-6}	2.269×10^{-6}
	0.4	1.765×10^{-4}	2.442×10^{-4}	1.683×10^{-4}	3.844×10^{-6}	6.398×10^{-6}	3.665×10^{-6}
	0.6	1.025×10^{-4}	1.434×10^{-4}	9.769×10^{-5}	1.029×10^{-5}	1.545×10^{-5}	9.806×10^{-6}
	0.8	3.666×10^{-5}	5.292×10^{-5}	3.495×10^{-5}	5.069×10^{-6}	8.448×10^{-6}	4.833×10^{-6}
	1	8.111×10^{-7}	1.714×10^{-6}	7.733×10^{-7}	5.708×10^{-7}	7.934×10^{-7}	5.443×10^{-7}

Table 12. *Cont.*

RBFs	t	$\alpha = 0.75$			$\alpha = 1$		
		L_2	L_∞	L_{rms}	L_2	L_∞	L_{rms}
			c = 6.73987			c = 8.05516	
IQ	0.2	1.874×10^{-4}	2.569×10^{-4}	1.787×10^{-4}	6.647×10^{-6}	8.712×10^{-6}	6.337×10^{-6}
	0.4	3.295×10^{-4}	4.515×10^{-4}	3.141×10^{-4}	2.459×10^{-5}	3.395×10^{-5}	2.344×10^{-5}
	0.6	3.312×10^{-4}	4.562×10^{-4}	3.157×10^{-4}	5.053×10^{-5}	6.511×10^{-5}	4.817×10^{-5}
	0.8	1.167×10^{-4}	1.641×10^{-4}	1.112×10^{-4}	1.887×10^{-4}	2.612×10^{-4}	1.799×10^{-4}
	1	3.197×10^{-6}	4.250×10^{-6}	3.048×10^{-6}	1.895×10^{-6}	3.064×10^{-6}	1.806×10^{-6}
			c = 0.333513			c = 0.22009	
GS	0.2	1.039×10^{-5}	1.683×10^{-5}	9.904×10^{-6}	3.868×10^{-5}	5.120×10^{-5}	3.688×10^{-5}
	0.4	2.716×10^{-4}	3.860×10^{-4}	2.589×10^{-4}	1.255×10^{-4}	1.707×10^{-4}	1.197×10^{-4}
	0.6	3.887×10^{-4}	5.566×10^{-4}	3.706×10^{-4}	1.440×10^{-4}	1.978×10^{-4}	1.373×10^{-4}
	0.8	1.526×10^{-4}	2.234×10^{-4}	1.455×10^{-4}	8.383×10^{-5}	1.163×10^{-4}	7.993×10^{-5}
	1	5.527×10^{-6}	1.015×10^{-5}	5.270×10^{-6}	6.293×10^{-6}	9.884×10^{-6}	6.000×10^{-6}

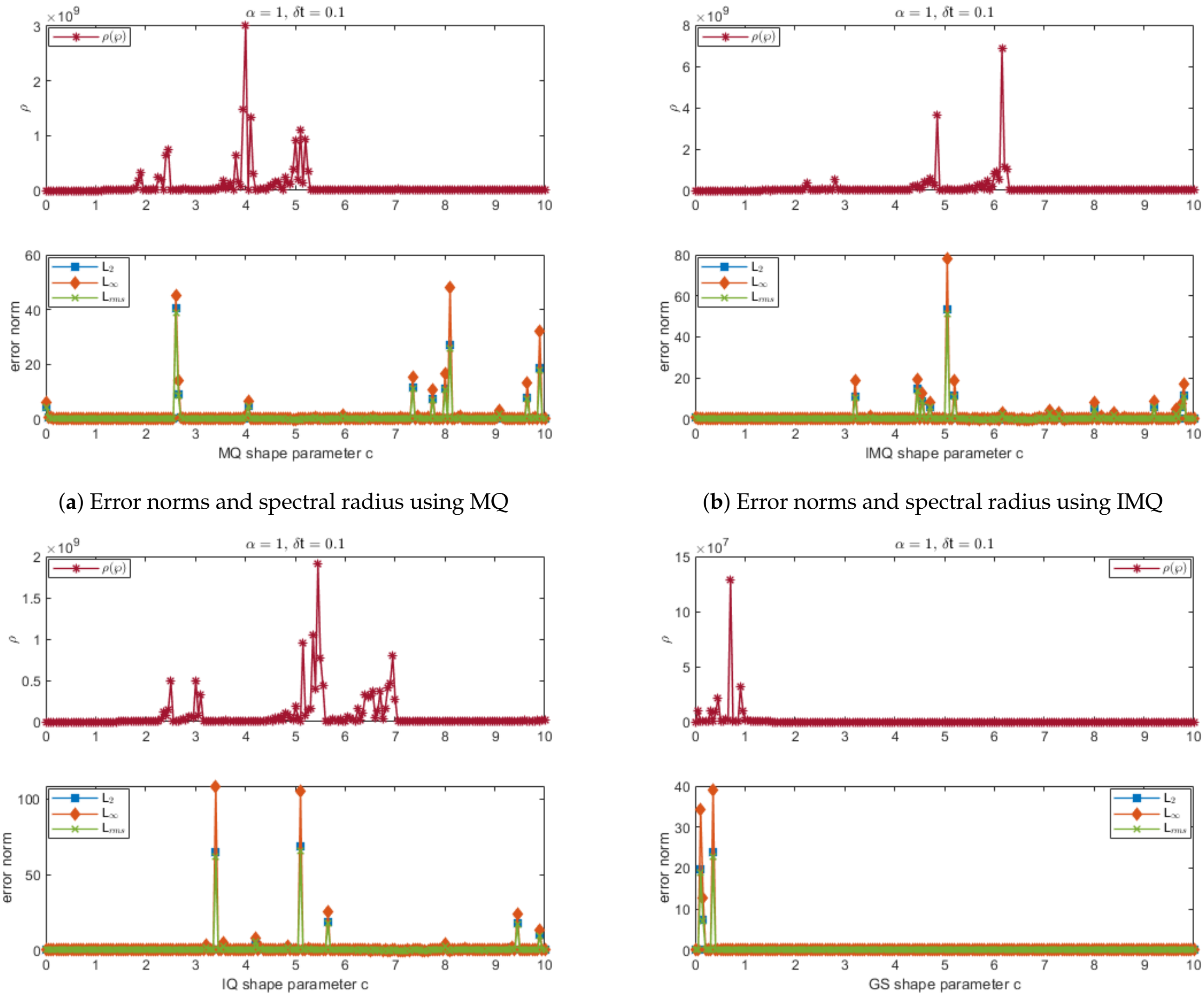

(**a**) Error norms and spectral radius using MQ (**b**) Error norms and spectral radius using IMQ

(**c**) Error norms and spectral radius against IQ (**d**) Error norms and spectral radius using GS

Figure 17. Error norms and spectral radius correspond to Example 3 when N = M = 10, $\alpha = 1$ using MQ, IMQ, IQ, and GS RBFs.

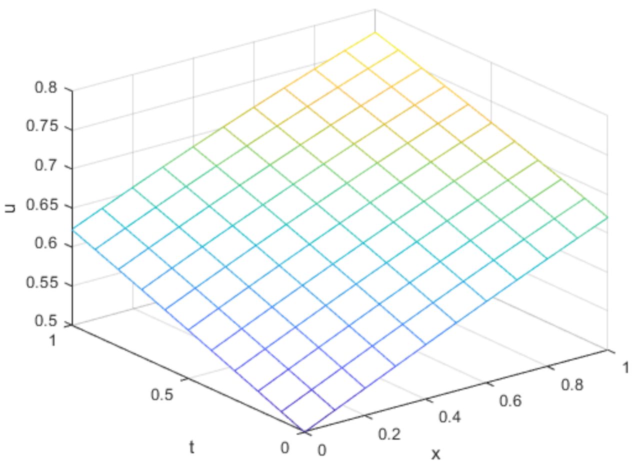

(**a**) Exact solution

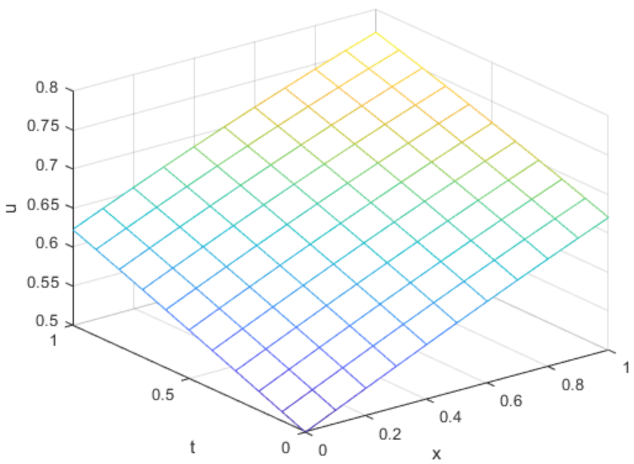

(**b**) Computed solution using MQ

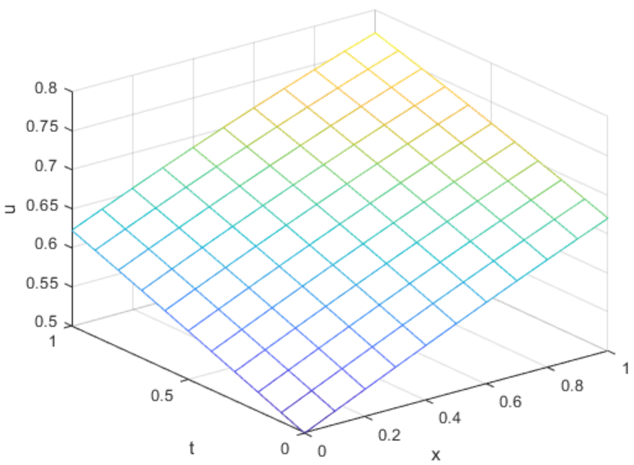

(**c**) Computed solution using IMQ

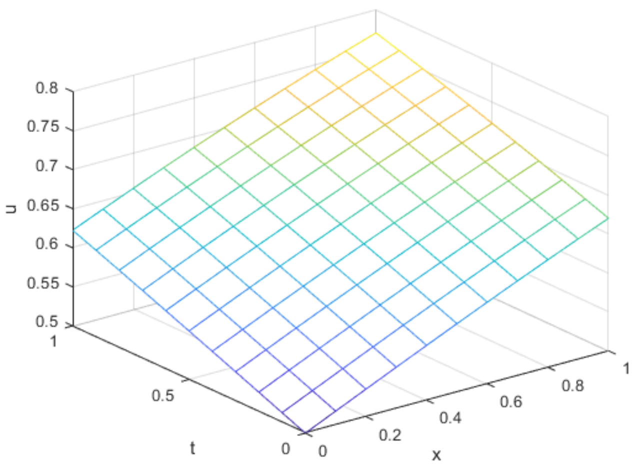

(**d**) Computed solution against IQ

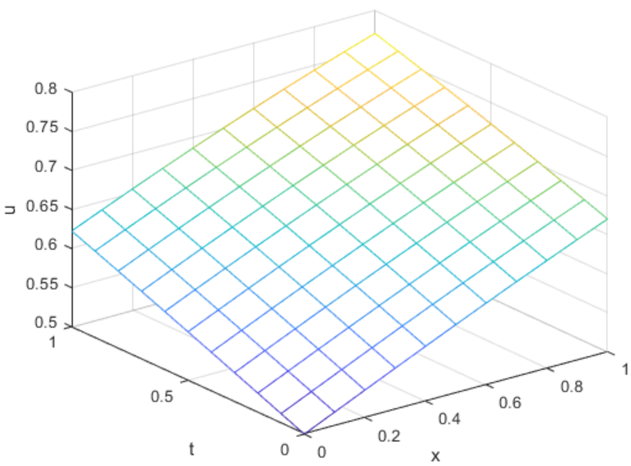

(**e**) Computed solution using GS

Figure 18. Exact vs. computed solution corresponds to Example 3 when $\mathrm{N} = \mathrm{M} = 10$, $\alpha = 1$ using MQ, IMQ, IQ, and GS RBFs.

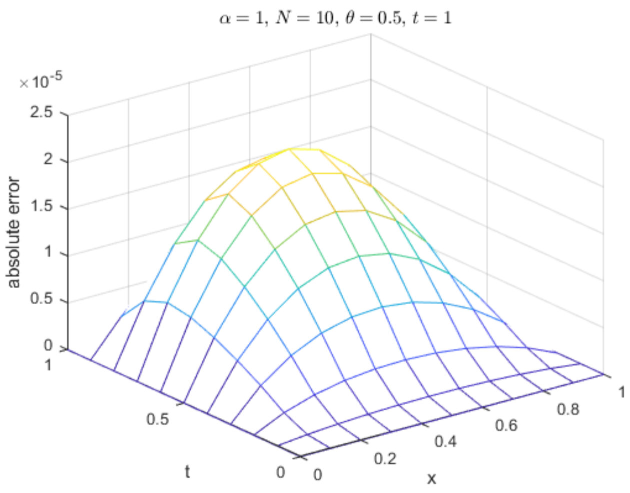

(**a**) Absolute error using MQ

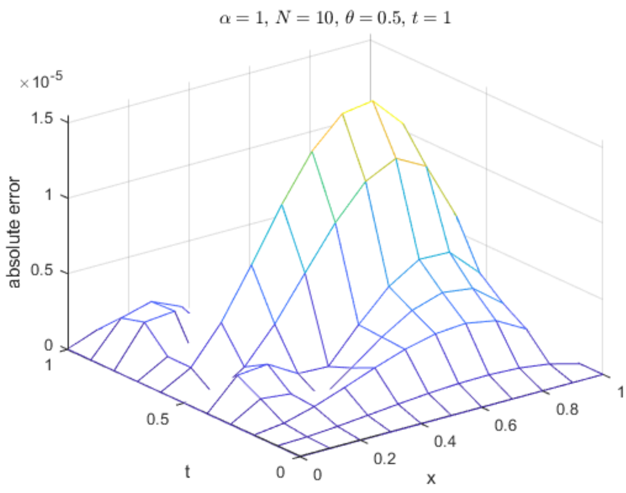

(**b**) Absolute error using IMQ

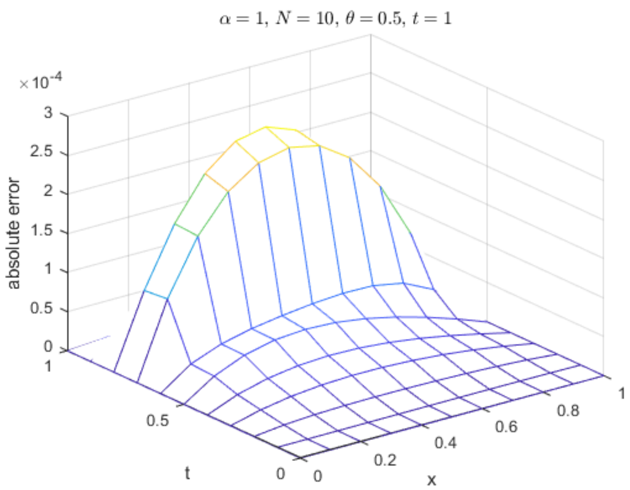

(**c**) Absolute error against IQ

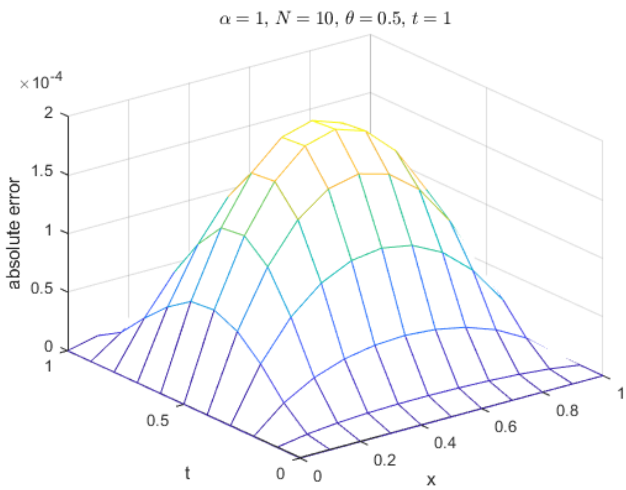

(**d**) Absolute error using GS

Figure 19. Absolute error of MQ, IMQ, IQ, and GS at t = 1 $\times$ 10^{-4} corresponds to Example 3.

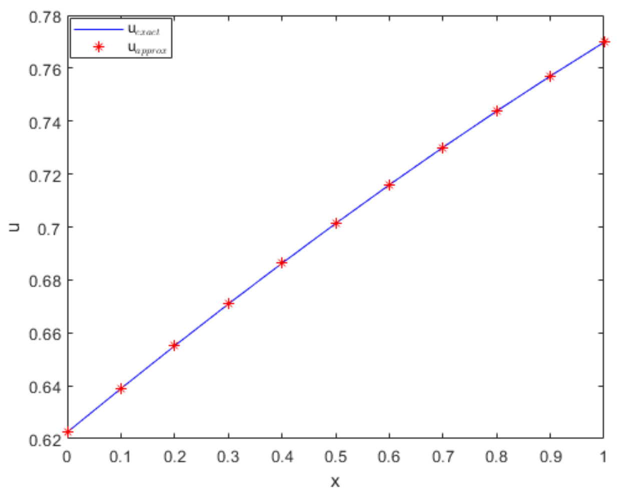

(**a**) Exact vs. numerical using MQ

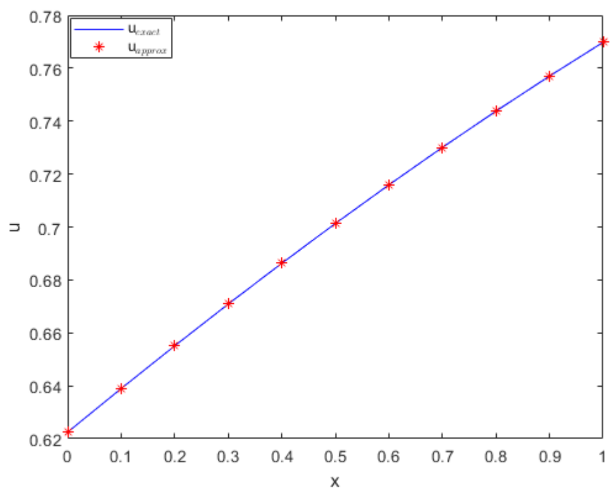

(**b**) Exact vs. numerical using IMQ

Figure 20. *Cont*.

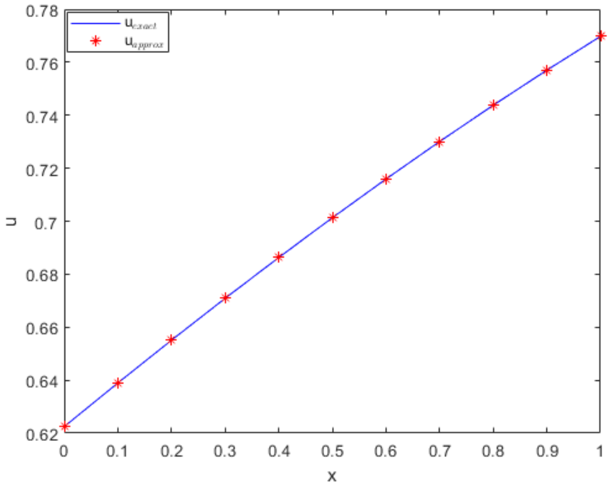

(**c**) Exact vs. numerical against IQ

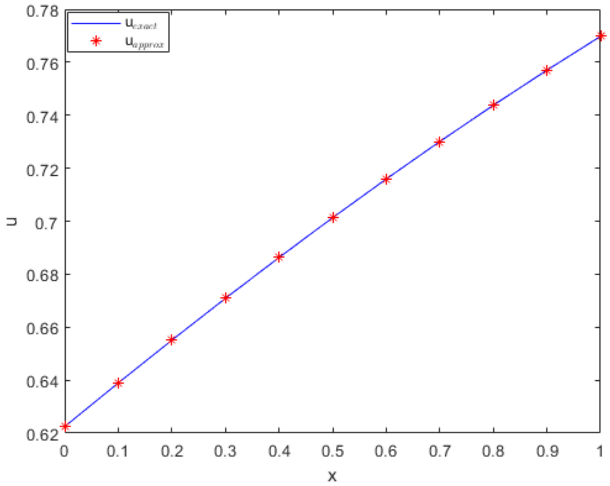

(**d**) Exact vs. numerical using GS

Figure 20. Comparison of exact and computed solution corresponds to Example 3 at t = 1 $\times$ 10^{-4} and $\alpha = 1$ using MQ, IMQ, IQ, and GS RBFs.

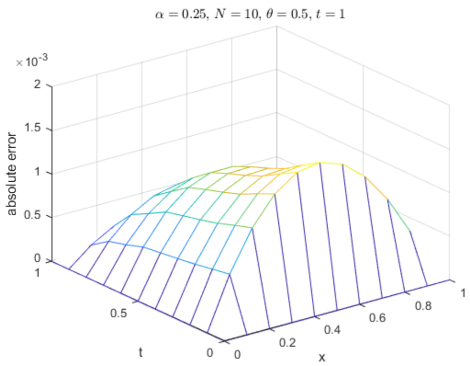

(**a**) Absolute error

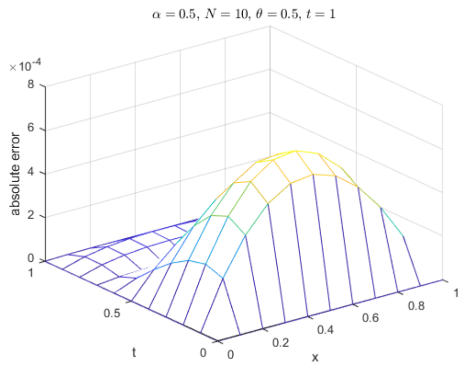

(**b**) Absolute error

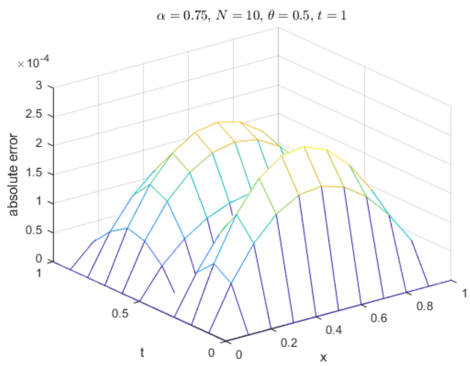

(**c**) Absolute error

Figure 21. Absolute errors for Example 3 with different values of α's using MQ RBF.

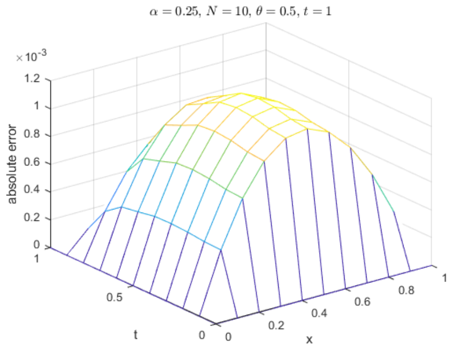

(**a**) Absolute error

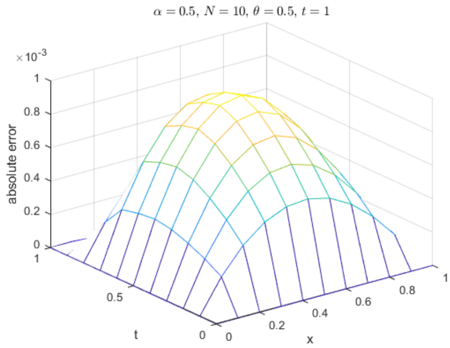

(**b**) Absolute error

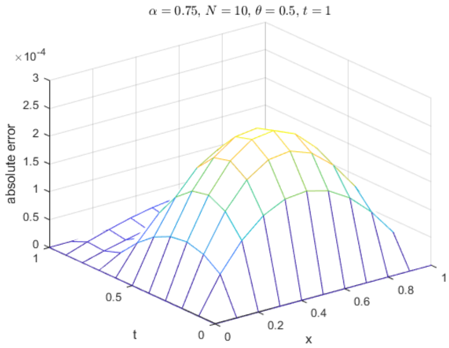

(**c**) Absolute error

Figure 22. Absolute errors for Example 3 with different values of α's using IMQ RBF.

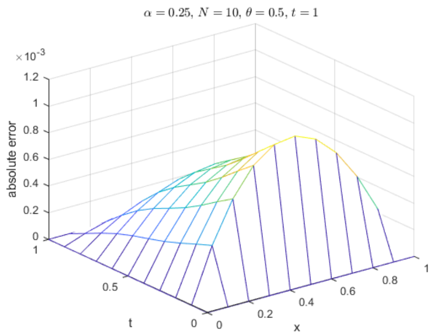

(**a**) Absolute error

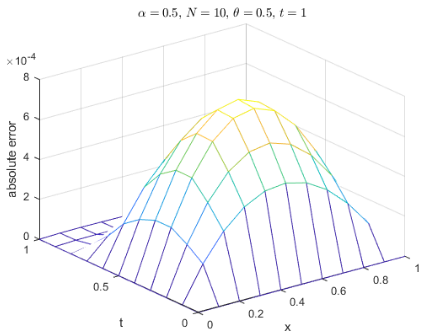

(**b**) Absolute error

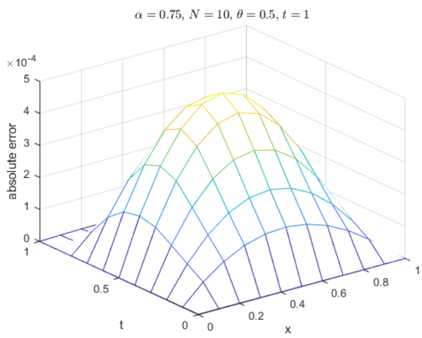

(**c**) Absolute error

Figure 23. Absolute errors for Example 3 with different values of α's using IQ RBF.

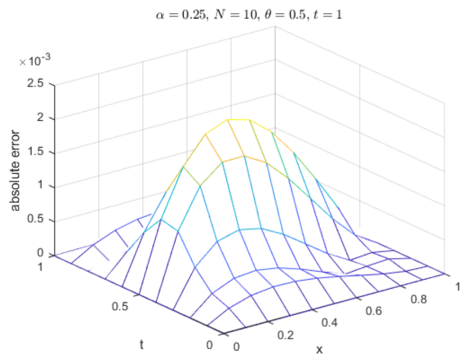

(**a**) Absolute error

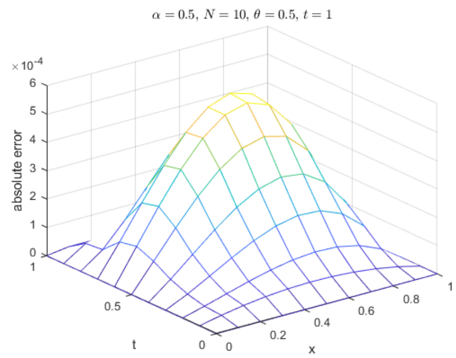

(**b**) Absolute error

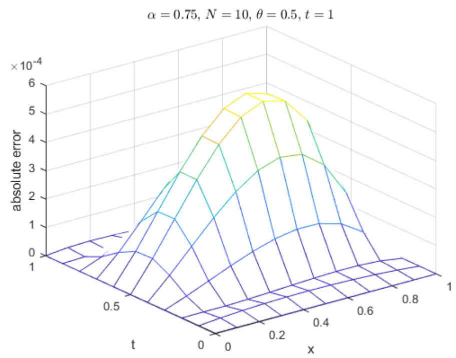

(**c**) Absolute error

Figure 24. Absolute errors for Example 3 with different values of α's using GS RBF.

Example 4. *Let us consider FitzHugh–Nagumo Equations (2) and (3). For $\alpha = 1$, the exact solution, as given in [27], is described by the following expression:*

$$u(t,x) = \frac{1}{1 + e^{\left(\frac{-x}{\sqrt{2}} + yt\right)}}, \quad \text{where} \quad y = \frac{1}{\sqrt{2}} - \sqrt{2}\beta,$$

where β represents an arbitrary constant. We employ the ICs and BCs from this exact solution. Using this solution, we apply the present method to approximate the exact solution within the domain $x \in [0,1]$. RBFs such as MQ, IMQ, IQ, and GS are employed for the numerical approximation. We choose $N = 10$, $\delta t = 0.001$, $\theta = 0.5$, and $\beta = -1$. The obtained results, in terms of absolute errors, are presented in Table 13 for $\alpha = 1$. The table clearly indicates that the accuracy of the present method is better than that of the homotopy perturbation transform technique (HPTT). Additionally, the comparison of the present method with HPTT is presented in Table 14 for $\beta = 0.45$ and $\alpha = 0.5$ while keeping the other parameters the same. The comparison shows that the results of the present method using different RBFs are more accurate than those of HPTT. Furthermore, the error norms at various time levels are recorded in Tables 15 and 16 for α values of 0.5 and 1 using the MQ, IMQ, IQ, and GS RBFs.

The stability and error norm plots are presented in Figures 25 and 26 for $\alpha = 1$ and 0.5 and $\beta = -1$ and $\beta = 0.45$, respectively, for $N = 10$, $\theta = 0.5$, and $\delta t = 0.001$, demonstrating that the present method consistently satisfies the Lax–Richtmyer stability criterion. Additionally, the surface plots in Figures 27 and 28 show that the computed solution using the selected RBFs closely matches the exact solution. The absolute errors for $\alpha = 1$ and 0.5 at various time levels are depicted in Figures 29 and 30, respectively, indicating reasonable accuracy. Finally, Figures 31 and 32 compare the exact and computed solutions at the final time, demonstrating the good accuracy of the present method.

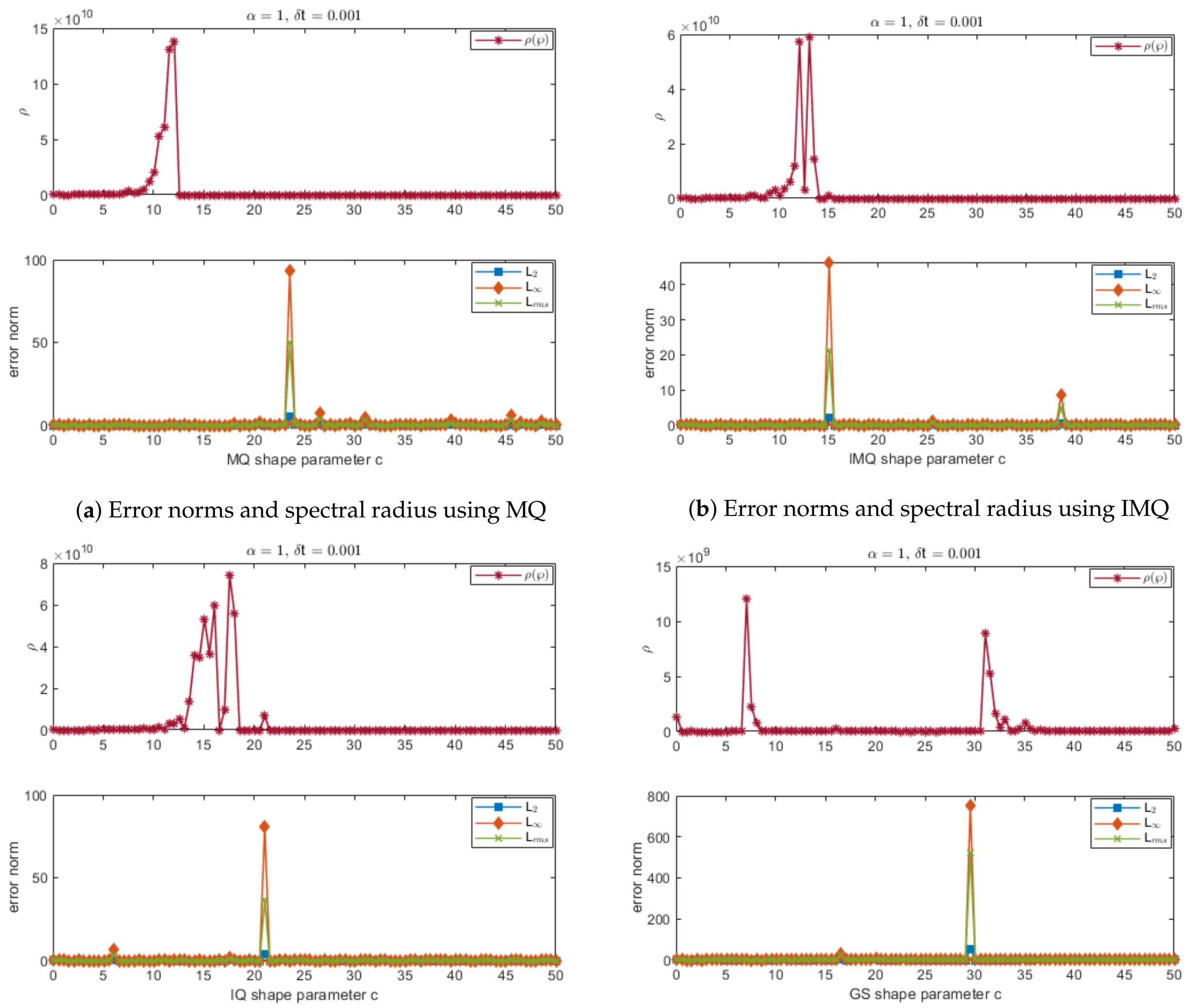

(**a**) Error norms and spectral radius using MQ

(**b**) Error norms and spectral radius using IMQ

(**c**) Error norms and spectral radius against IQ

(**d**) Error norms and spectral radius using GS

Figure 25. Error norms and spectral radius correspond to Example 4 when $N = M = 10$, $\alpha = 1$ using MQ, IMQ, IQ, and GS RBFs.

Table 13. Comparison of absolute errors of the present method solution with HPTT using MQ, IMQ, IQ, and GS RBFs for $\alpha = 1$, $\beta = -1$, $N = 10$, $\theta = 0.5$, and $\delta t = 0.001$ corresponds to Example 4.

x	**t**	[27]	**MQ**	**IMQ**	**IQ**	**GS**
			c = 18.6452	**c = 15.3437**	**c = 19.0984**	**c = 0.3839**
0.001	0.001	1.5×10^{-3}	2.604×10^{-9}	1.507×10^{-9}	1.243×10^{-9}	1.019×10^{-9}
0.002	0.002	3.0×10^{-3}	1.287×10^{-8}	3.875×10^{-9}	4.379×10^{-9}	8.782×10^{-11}
0.003	0.003	4.5×10^{-3}	1.573×10^{-8}	1.229×10^{-8}	9.328×10^{-9}	1.306×10^{-9}
0.004	0.004	6.0×10^{-3}	9.833×10^{-9}	6.037×10^{-9}	9.718×10^{-9}	3.324×10^{-9}
0.005	0.005	7.5×10^{-3}	1.269×10^{-8}	7.529×10^{-9}	2.312×10^{-8}	4.515×10^{-9}
0.006	0.006	9.1×10^{-3}	9.864×10^{-9}	6.832×10^{-9}	3.217×10^{-9}	5.898×10^{-9}
0.007	0.007	1.0×10^{-2}	2.049×10^{-9}	5.261×10^{-9}	6.513×10^{-9}	1.112×10^{-8}
0.008	0.008	1.2×10^{-2}	4.631×10^{-10}	5.446×10^{-9}	4.356×10^{-10}	1.287×10^{-8}
0.009	0.009	1.3×10^{-2}	3.879×10^{-9}	5.513×10^{-11}	1.102×10^{-9}	6.502×10^{-9}
0.010	0.010	1.5×10^{-2}	9.973×10^{-10}	8.579×10^{-10}	1.403×10^{-10}	1.438×10^{-9}

Table 14. Comparison of absolute errors of the present method solution with HPTT using MQ, IMQ, IQ, and GS RBFs for $\alpha = 0.5$, $\beta = 0.45$, $N = 10$, $\theta = 0.5$, and $\delta t = 0.001$ corresponds to Example 4.

x	t	[27]	MQ	IMQ	IQ	GS
			c = 5.8849	**c = 46.8122**	**c = 21.9648**	**c = 0.01313**
0.001	0.001	2.8×10^{-2}	5.428×10^{-10}	2.256×10^{-9}	8.790×10^{-11}	8.717×10^{-10}
0.002	0.002	4.1×10^{-2}	3.680×10^{-10}	2.810×10^{-9}	3.522×10^{-10}	4.335×10^{-10}
0.003	0.003	5.3×10^{-2}	6.547×10^{-10}	2.313×10^{-9}	2.294×10^{-12}	1.436×10^{-8}
0.004	0.004	6.2×10^{-2}	3.745×10^{-10}	4.687×10^{-9}	1.209×10^{-9}	6.656×10^{-9}
0.005	0.005	6.9×10^{-2}	2.766×10^{-10}	1.804×10^{-9}	5.891×10^{-10}	1.806×10^{-9}
0.006	0.006	8.0×10^{-2}	5.124×10^{-11}	4.929×10^{-9}	1.687×10^{-9}	4.174×10^{-9}
0.007	0.007	8.7×10^{-2}	2.419×10^{-11}	5.098×10^{-10}	1.065×10^{-9}	2.086×10^{-9}
0.008	0.008	9.4×10^{-2}	3.764×10^{-11}	8.220×10^{-10}	2.522×10^{-10}	3.540×10^{-10}
0.009	0.009	1.0×10^{-2}	2.451×10^{-11}	3.408×10^{-10}	1.441×10^{-9}	7.412×10^{-10}
0.010	0.010	1.1×10^{-2}	1.957×10^{-11}	4.644×10^{-10}	9.778×10^{-11}	1.064×10^{-9}

Table 15. Error norms at various time levels using MQ, IMQ, IQ, and GS RBFs for $\beta = -1$, $N = 10$, $\theta = 0.5$, and $\delta t = 0.001$ corresponds to Example 4.

RBFs	t	$\alpha = 0.5$			$\alpha = 1$		
		L_2	L_∞	L_{rms}	L_2	L_∞	L_{rms}
MQ		c = 2.2759			c = 18.6452		
	0.002	1.826×10^{-9}	2.695×10^{-8}	1.741×10^{-8}	1.506×10^{-9}	2.005×10^{-8}	1.436×10^{-8}
	0.004	3.987×10^{-10}	7.487×10^{-9}	3.801×10^{-9}	8.064×10^{-10}	1.239×10^{-8}	7.688×10^{-9}
	0.006	3.952×10^{-10}	6.265×10^{-9}	3.768×10^{-9}	7.224×10^{-10}	9.868×10^{-9}	6.888×10^{-9}
	0.008	1.206×10^{-10}	2.755×10^{-9}	1.150×10^{-9}	1.338×10^{-10}	2.402×10^{-9}	1.276×10^{-9}
	0.01	8.903×10^{-11}	1.567×10^{-9}	8.488×10^{-10}	8.692×10^{-11}	1.269×10^{-9}	8.287×10^{-10}
IMQ		c = 35.2365			c = 15.3437		
	0.002	1.410×10^{-9}	2.428×10^{-8}	1.344×10^{-8}	5.814×10^{-10}	9.810×10^{-9}	5.543×10^{-9}
	0.004	9.698×10^{-10}	1.670×10^{-8}	9.247×10^{-9}	3.875×10^{-10}	7.351×10^{-9}	3.695×10^{-9}
	0.006	2.074×10^{-9}	3.516×10^{-8}	1.977×10^{-8}	5.499×10^{-10}	7.665×10^{-9}	5.243×10^{-9}
	0.008	1.188×10^{-9}	1.630×10^{-8}	1.133×10^{-8}	5.216×10^{-10}	7.340×10^{-9}	4.973×10^{-9}
	0.01	7.080×10^{-10}	1.068×10^{-8}	6.751×10^{-9}	1.326×10^{-10}	2.486×10^{-9}	1.264×10^{-9}
IQ		c = 22.2965			c = 19.0984		
	0.002	4.624×10^{-9}	6.265×10^{-8}	4.409×10^{-8}	4.838×10^{-10}	6.599×10^{-9}	4.613×10^{-9}
	0.004	9.319×10^{-9}	1.256×10^{-7}	8.885×10^{-8}	7.086×10^{-10}	1.217×10^{-8}	6.757×10^{-9}
	0.006	2.882×10^{-9}	5.671×10^{-8}	2.748×10^{-8}	6.541×10^{-10}	1.277×10^{-8}	6.237×10^{-9}
	0.008	5.201×10^{-9}	7.886×10^{-8}	4.959×10^{-8}	1.535×10^{-10}	3.069×10^{-9}	1.463×10^{-9}
	0.01	1.441×10^{-9}	2.486×10^{-8}	1.374×10^{-8}	7.404×10^{-11}	1.420×10^{-9}	7.059×10^{-10}
GS		c = 0.2654			c = 0.3839		
	0.002	2.842×10^{-9}	3.915×10^{-8}	2.710×10^{-8}	1.096×10^{-10}	1.716×10^{-9}	1.045×10^{-9}
	0.004	5.743×10^{-9}	7.859×10^{-8}	5.476×10^{-8}	2.960×10^{-10}	4.213×10^{-9}	2.822×10^{-9}
	0.006	4.834×10^{-9}	7.845×10^{-8}	4.609×10^{-8}	4.196×10^{-10}	5.898×10^{-9}	4.001×10^{-9}
	0.008	5.551×10^{-9}	1.224×10^{-7}	5.292×10^{-8}	1.245×10^{-9}	1.639×10^{-8}	1.187×10^{-8}
	0.01	1.994×10^{-9}	3.734×10^{-8}	1.901×10^{-8}	1.991×10^{-10}	2.787×10^{-9}	1.898×10^{-9}

Table 16. Error norms at various time levels using MQ, IMQ, IQ, and GS RBFs for $\beta = 0.45$, N = 10, $\theta = 0.5$, and $\delta t = 0.001$ correspond to Example 4.

RBFs	t	$\alpha = 0.5$			$\alpha = 1$		
		L_2	L_∞	L_{rms}	L_2	L_∞	L_{rms}
		c = 5.8849			c = 4.46		
MQ	0.002	3.997×10^{-11}	6.588×10^{-10}	3.811×10^{-10}	3.832×10^{-11}	5.612×10^{-10}	3.654×10^{-10}
	0.004	2.543×10^{-11}	4.185×10^{-10}	2.425×10^{-10}	4.074×10^{-11}	6.447×10^{-10}	3.885×10^{-10}
	0.006	2.687×10^{-11}	4.331×10^{-10}	2.562×10^{-10}	3.552×10^{-11}	5.081×10^{-10}	3.387×10^{-10}
	0.008	2.878×10^{-11}	5.097×10^{-10}	2.744×10^{-10}	1.383×10^{-11}	1.986×10^{-10}	1.318×10^{-10}
	0.01	1.573×10^{-11}	2.450×10^{-10}	1.500×10^{-10}	9.560×10^{-12}	1.679×10^{-10}	9.115×10^{-11}
		c = 46.8122			c = 47.0019		
IMQ	0.002	1.732×10^{-10}	2.901×10^{-9}	1.652×10^{-9}	4.734×10^{-11}	7.761×10^{-10}	4.513×10^{-10}
	0.004	3.925×10^{-10}	5.261×10^{-9}	3.742×10^{-9}	4.022×10^{-11}	7.685×10^{-10}	3.835×10^{-10}
	0.006	3.585×10^{-10}	5.686×10^{-9}	3.418×10^{-9}	6.586×10^{-11}	1.284×10^{-9}	6.280×10^{-10}
	0.008	2.187×10^{-10}	3.579×10^{-9}	2.085×10^{-9}	7.760×10^{-11}	1.417×10^{-9}	7.399×10^{-10}
	0.01	4.236×10^{-11}	6.657×10^{-10}	4.038×10^{-10}	2.589×10^{-11}	3.952×10^{-10}	2.468×10^{-10}
		c = 21.9648			c = 15.2317		
IQ	0.002	2.981×10^{-11}	4.302×10^{-10}	2.842×10^{-10}	6.390×10^{-11}	1.053×10^{-9}	6.092×10^{-10}
	0.004	7.874×10^{-11}	1.499×10^{-9}	7.508×10^{-10}	4.657×10^{-11}	9.039×10^{-10}	4.441×10^{-10}
	0.006	1.340×10^{-10}	1.833×10^{-9}	1.278×10^{-9}	4.018×10^{-11}	7.631×10^{-10}	3.831×10^{-10}
	0.008	3.544×10^{-11}	6.846×10^{-10}	3.379×10^{-10}	1.035×10^{-10}	1.417×10^{-9}	9.868×10^{-10}
	0.01	4.529×10^{-11}	8.046×10^{-10}	4.318×10^{-10}	2.827×10^{-11}	4.326×10^{-10}	2.695×10^{-10}
		c = 0.01313			c = 0.17158		
GS	0.002	7.714×10^{-11}	1.385×10^{-9}	7.355×10^{-10}	1.530×10^{-11}	3.216×10^{-10}	1.459×10^{-10}
	0.004	1.041×10^{-9}	2.445×10^{-8}	9.924×10^{-9}	5.598×10^{-11}	7.387×10^{-10}	5.338×10^{-10}
	0.006	5.649×10^{-10}	9.973×10^{-9}	5.386×10^{-9}	3.017×10^{-11}	5.142×10^{-10}	2.876×10^{-10}
	0.008	2.462×10^{-10}	3.775×10^{-9}	2.348×10^{-9}	1.693×10^{-11}	2.656×10^{-10}	1.615×10^{-10}
	0.01	1.223×10^{-10}	1.844×10^{-9}	1.166×10^{-9}	2.405×10^{-11}	5.014×10^{-10}	2.293×10^{-10}

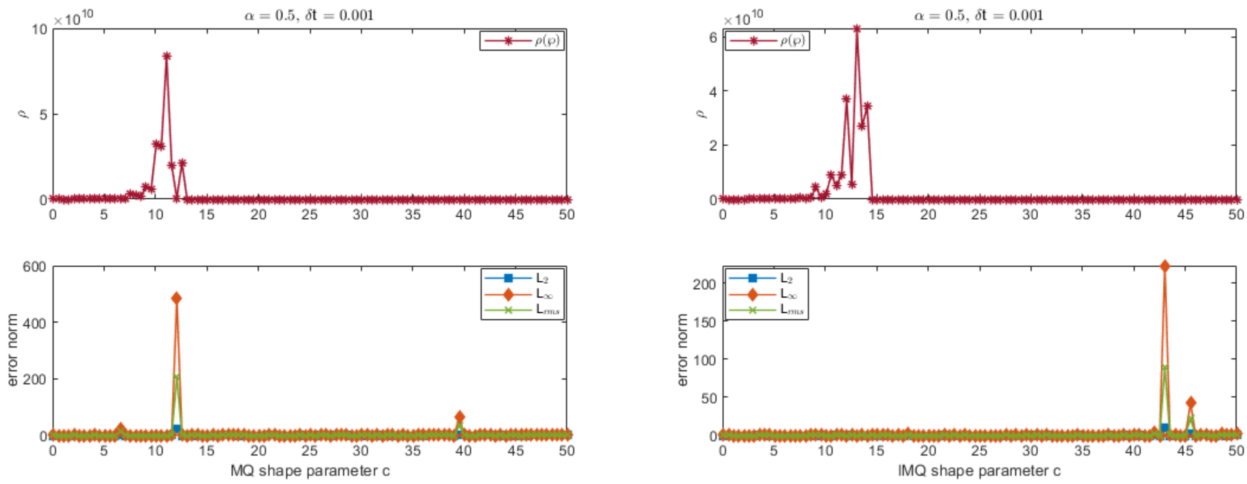

(**a**) Error norms and spectral radius using MQ (**b**) Error norms and spectral radius using IMQ

Figure 26. *Cont.*

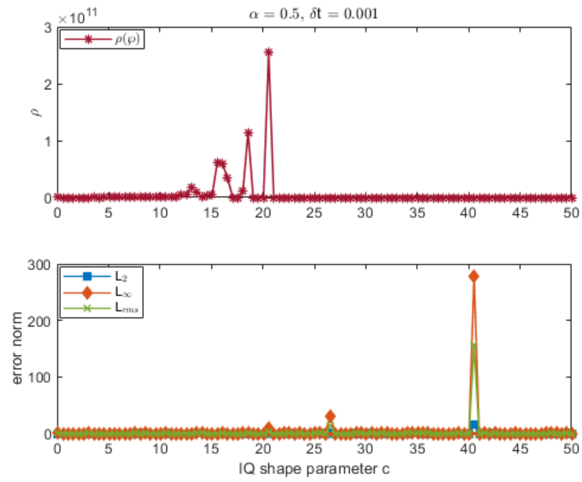

(**c**) Error norms and spectral radius against IQ

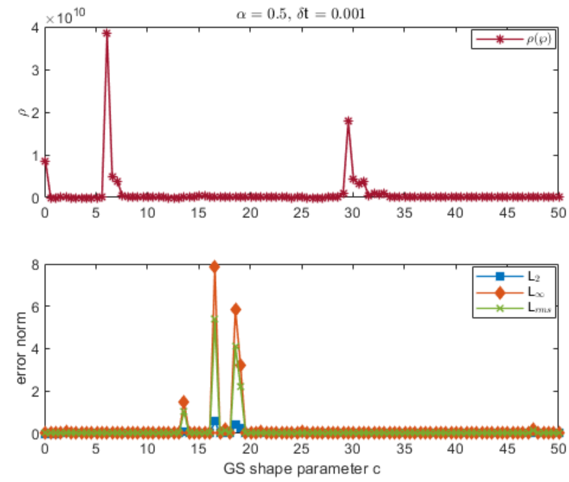

(**d**) Error norms and spectral radius using GS

Figure 26. Error norms and spectral radius correspond to Example 4 when $\mathrm{N} = \mathrm{M} = 10$, $\alpha = 0.5$ using MQ, IMQ, IQ, and GS RBFs.

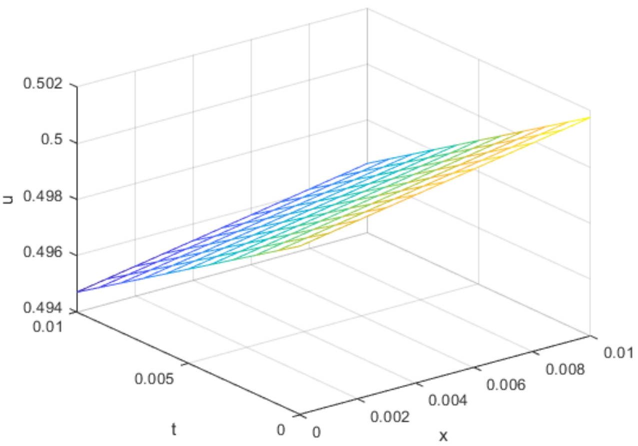

(**a**) Exact solution

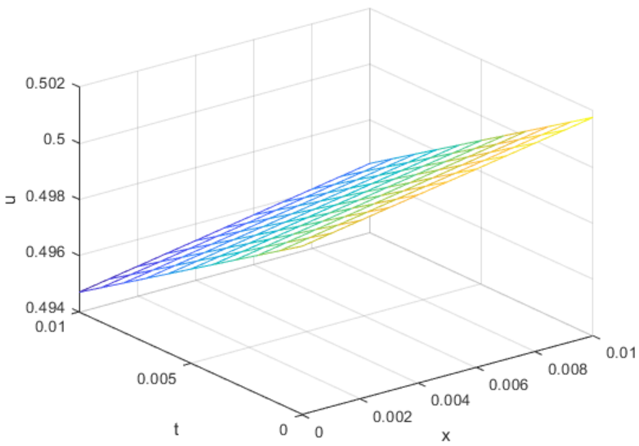

(**b**) Computed solution using MQ

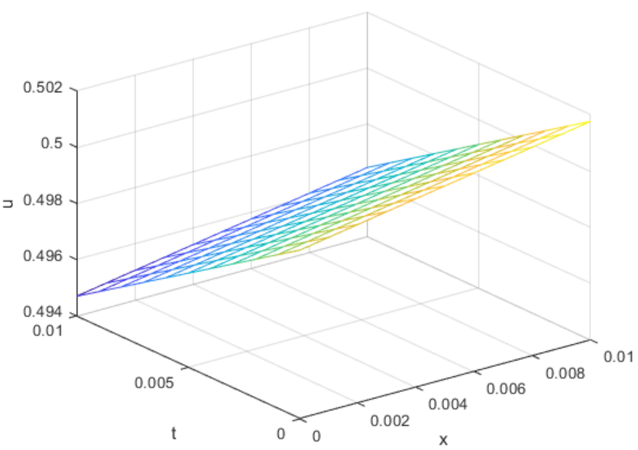

(**c**) Computed solution using IMQ

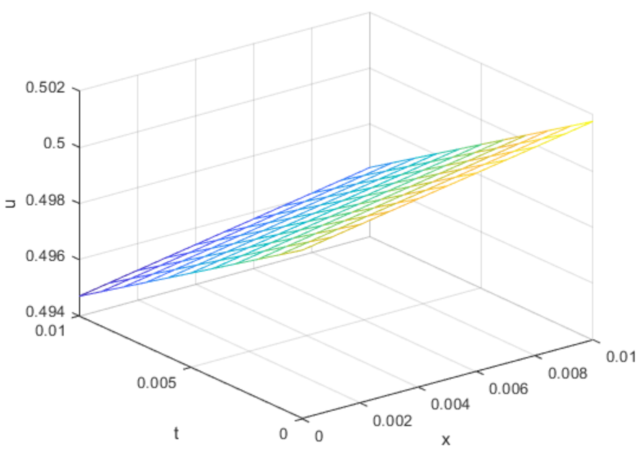

(**d**) Computed solution against IQ

Figure 27. *Cont.*

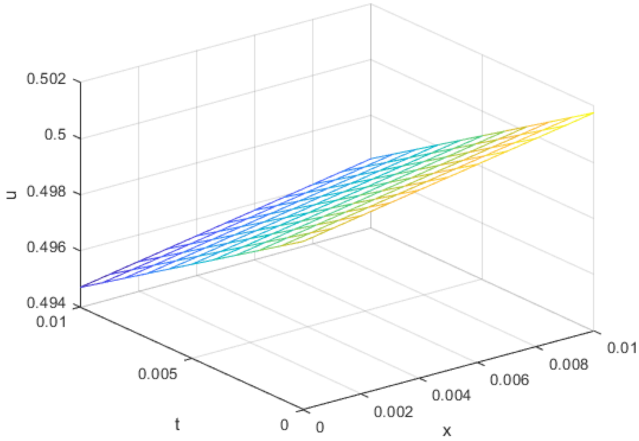

(**e**) Computed solution using GS

Figure 27. Exact vs. computed solution corresponds to Example 4 when N = M = 10, $\alpha = 1$ using MQ, IMQ, IQ, and GS RBFs.

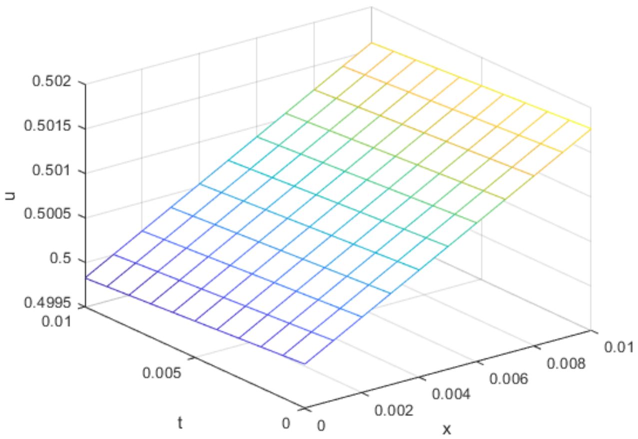

(**a**) Exact solution

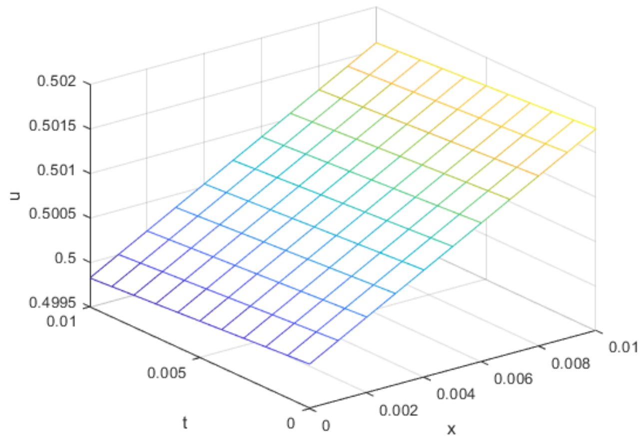

(**b**) Computed solution using MQ

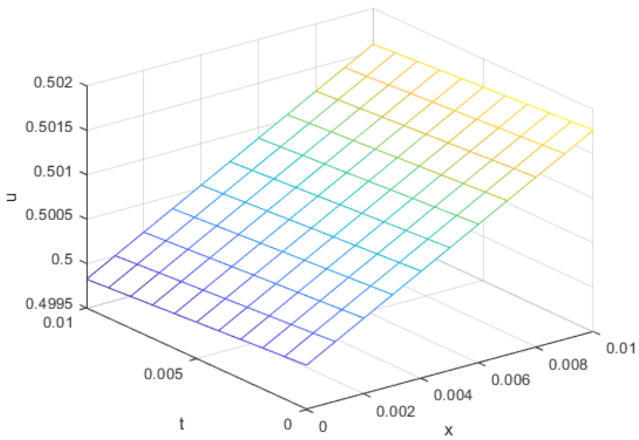

(**c**) Computed solution using IMQ

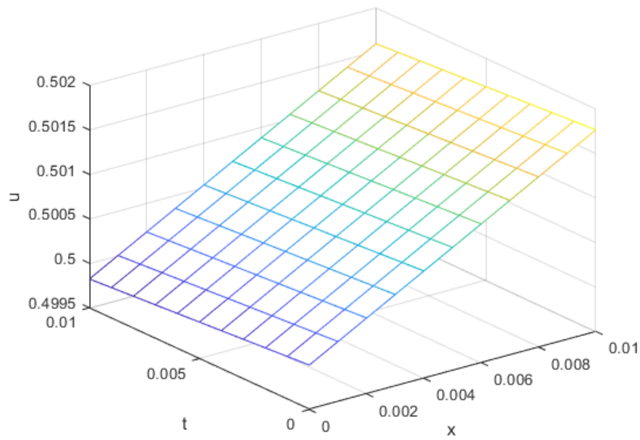

(**d**) Computed solution against IQ

Figure 28. *Cont*.

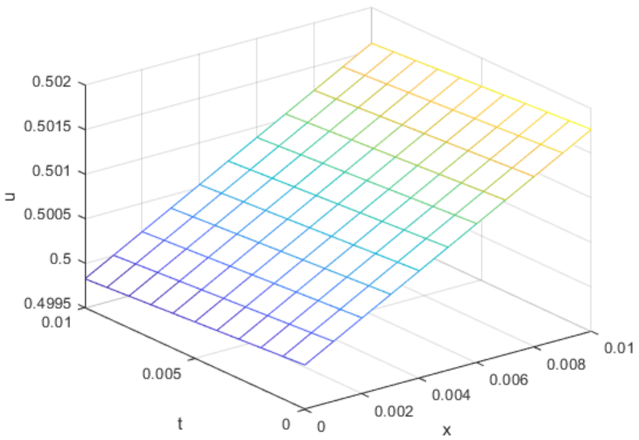

(**e**) Computed solution using GS

Figure 28. Exact vs. computed solution corresponds to Example 4 when N = M = 10, $\alpha = 0.5$ using MQ, IMQ, IQ, and GS RBFs.

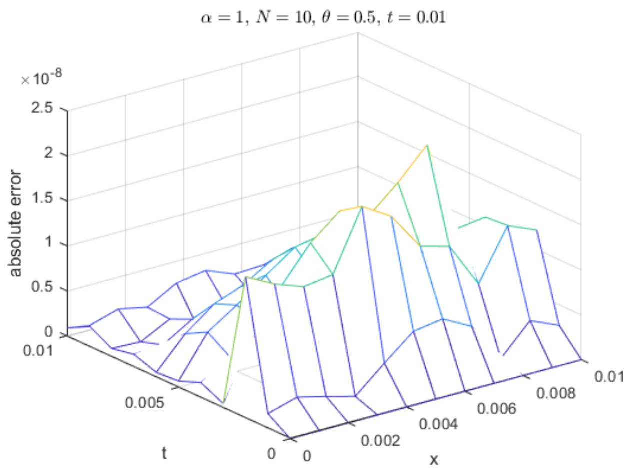

(**a**) Absolute error using MQ

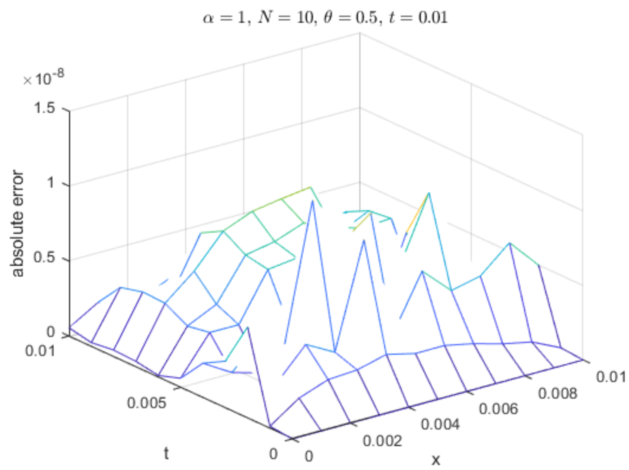

(**b**) Absolute error using IMQ

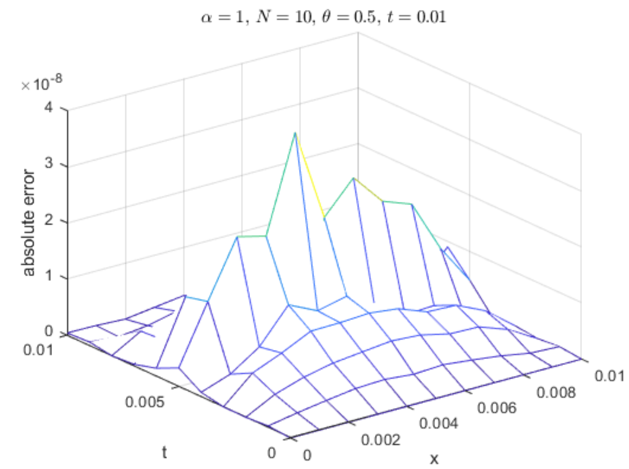

(**c**) Absolute error against IQ

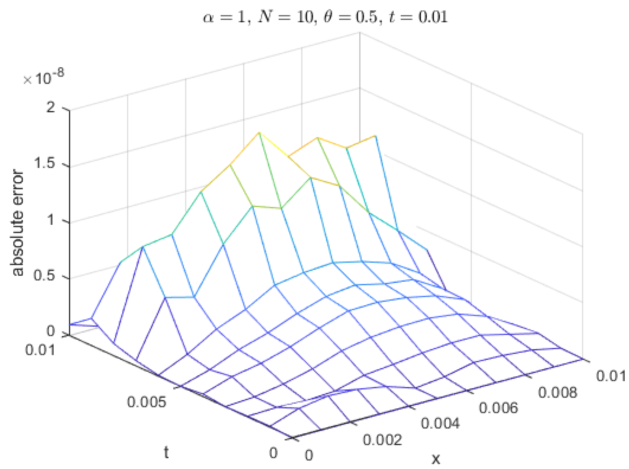

(**d**) Absolute error using GS

Figure 29. Absolute error of MQ, IMQ, IQ, and GS at t = 0.01 corresponds to Example 4.

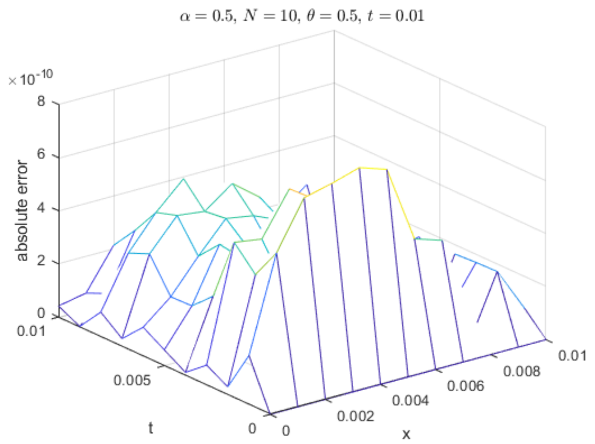

(**a**) Absolute error using MQ

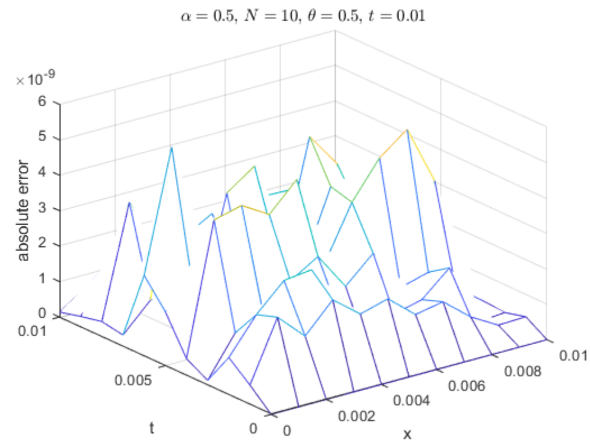

(**b**) Absolute error using IMQ

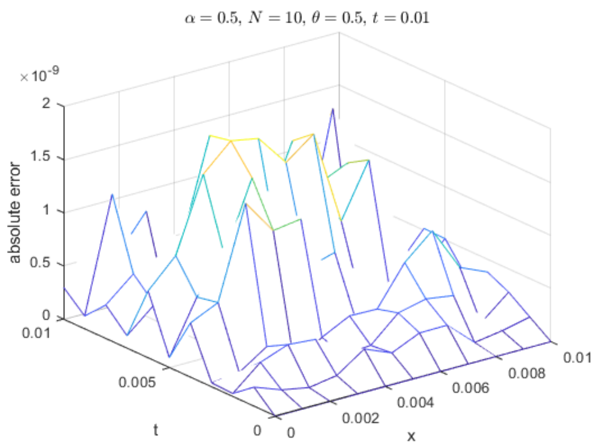

(**c**) Absolute error against IQ

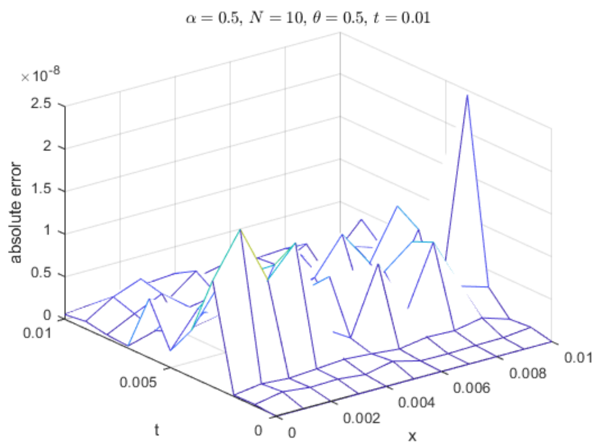

(**d**) Absolute error using GS

Figure 30. Absolute error of MQ, IMQ, IQ, and GS at t = 0.01 corresponds to Example 4.

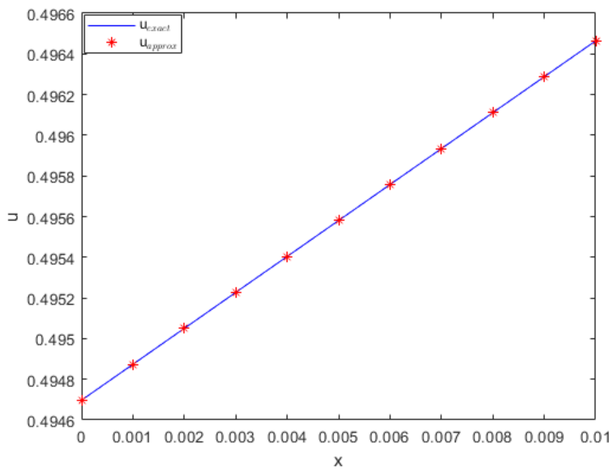

(**a**) Exact vs. numerical using MQ

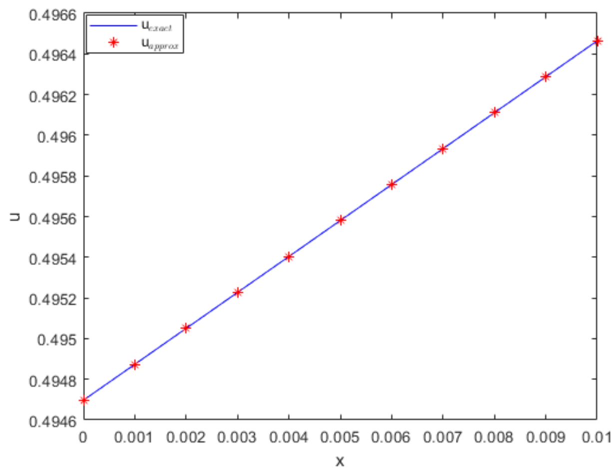

(**b**) Exact vs. numerical using IMQ

Figure 31. *Cont.*

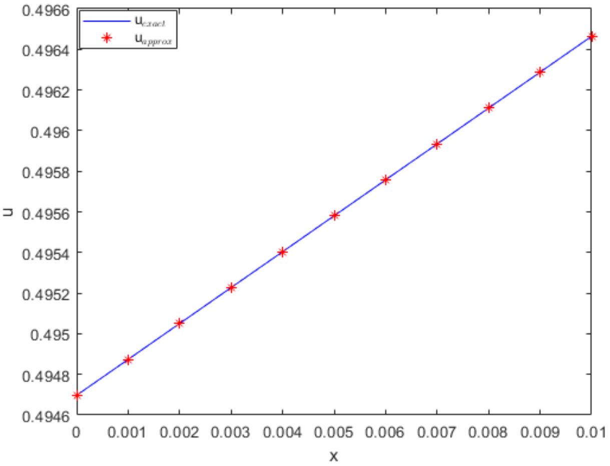

(**c**) Exact vs. numerical against IQ

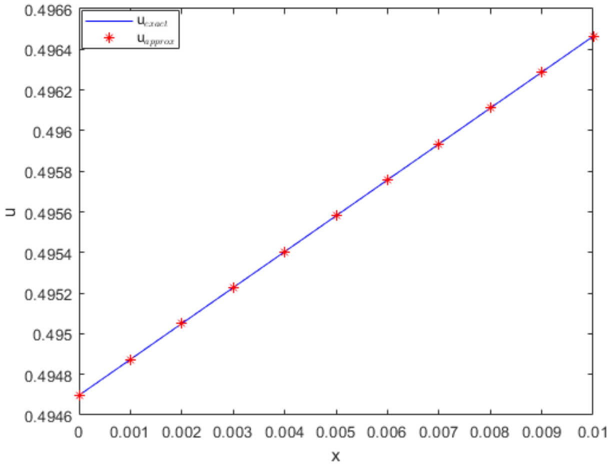

(**d**) Exact vs. numerical using GS

Figure 31. Comparison of exact and computed solution corresponds to Example 4 at t = 0.01 and $\alpha = 1$ using MQ, IMQ, IQ, and GS RBFs.

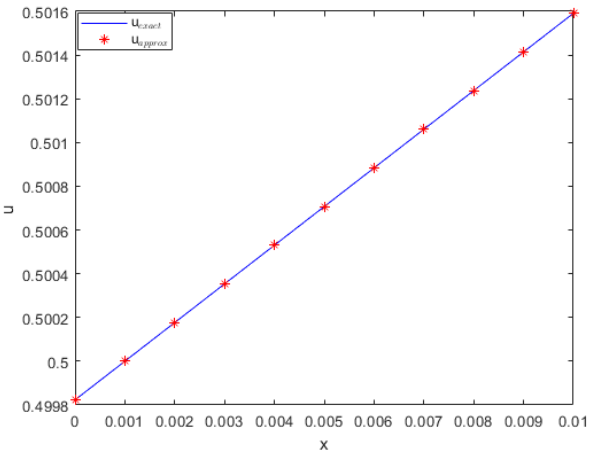

(**a**) Exact vs. numerical using MQ

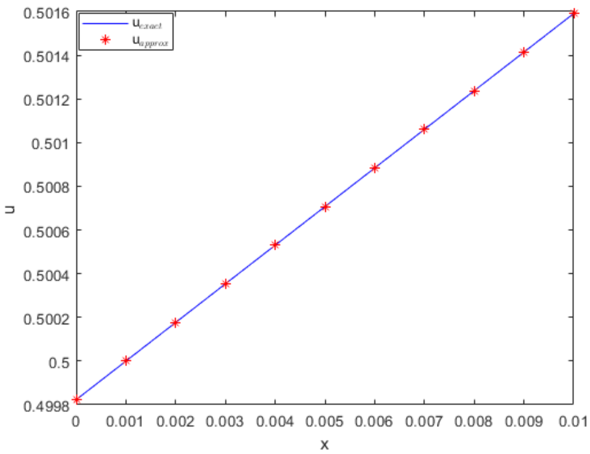

(**b**) Exact vs. numerical using IMQ

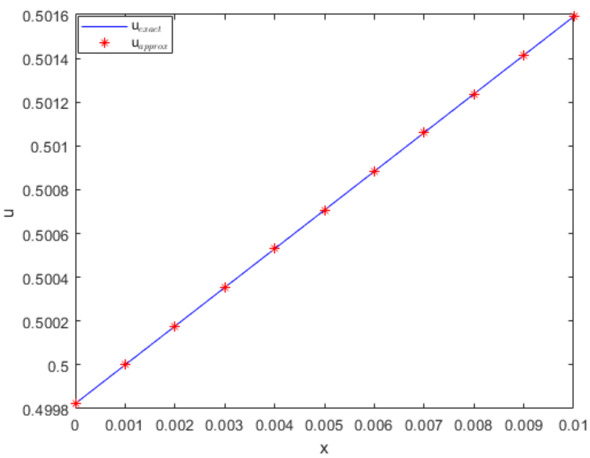

(**c**) Exact vs. numerical against IQ

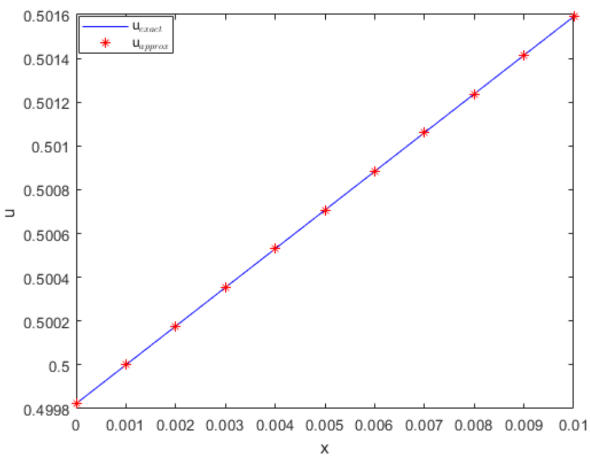

(**d**) Exact vs. numerical using GS

Figure 32. Comparison of exact and computed solution corresponds to Example 4 at t = 0.01 and $\alpha = 0.5$ using MQ, IMQ, IQ, and GS RBFs.

4. Conclusions

The RBF collocation method has been employed to numerically solve a range of FitzHugh–Nagumo Equations (2) and (3). The computed solutions exhibit excellent agreement with exact solutions across various parameter values. The accuracy of this method was rigorously assessed using different error norms. The results unequivocally establish that the proposed approach is highly effective in handling fractional PDE. Furthermore, the stability of the proposed algorithm was demonstrated through eigenvalue analysis, particularly focusing on the MQ, IMQ, IQ, and GS RBFs' shape parameter, denoted as c. From a computational standpoint, it is evident that the present method offers significant efficiency benefits, as it requires a minimal number of nodes and allows for fine-tuning of the RBF shape parameter to achieve satisfactory accuracy. Building on these achievements, several promising avenues for future research emerge.

- Investigate the use of locally supported RBFs to enhance adaptability to intricate spatial structures, improving accuracy in localized phenomena.
- Extend the methodology to incorporate time–space fractional derivatives, deepening understanding and expanding applicability to a broader range of real-world problems.
- The present study focuses on one-dimensional scenarios, and broadening its scope to handle multidimensional systems would significantly enhance its utility in practical applications.
- Exploring parallelization methods tailored for distributed memory systems would augment the adaptability and practical relevance of the presented techniques. Addressing these aspects not only demonstrates the methods' capacity to handle resource-intensive challenges but also enriches our understanding of their real-world applicability.

Author Contributions: Conceptualization, M.A.; methodology, M.A.; software, M.A., S.H., I.A., M.J.E. and S.S.; validation, M.A., S.H., I.A., M.J.E. and S.S.; formal analysis, M.A.; investigation, M.A.; writing—original draft preparation, M.A.; writing—review and editing, S.H., I.A., M.J.E. and S.S.; supervision, S.H.; funding acquisition, M.J.E. All authors have read and agreed to the published version of the manuscript.

Funding: This research received no external funding.

Data Availability Statement: The data used to support the findings of this study are available from the first author upon request.

Acknowledgments: The first author would like to express gratitude to the GIK Institute for their support during his MS studies. The authors would like to express their sincere thanks to the Department of Mathematics, Chabahar Maritime University, Chabahar, Iran, for the financial support.

Conflicts of Interest: The authors declare that they have no conflict of interest.

References

1. Bhrawy, A.H. A Jacobi–Gauss–Lobatto collocation method for solving generalized Fitzhugh–Nagumo equation with time-dependent coefficients. *Appl. Math. Comput.* **2013**, *222*, 255–264. [CrossRef]
2. Fitzhugh, R. Impulses and physiological states in models of nerve membrane. *Biophys. J.* **1961**, *1*, 445–466. [CrossRef]
3. Nagumo, J.; Arimoto, S.; Yoshizawa, S. An active pulse transmission line simulating nerve axon. *Proc. Ire* **1962**, *50*, 2061–2070. [CrossRef]
4. Shih, M.; Momoniat, E.; Mahomed, F. Approximate conditional symmetries and approximate solutions of the perturbed Fitzhugh–Nagumo equation. *J. Math. Phys.* **2005**, *46*, 023503. [CrossRef]
5. Kawahara, T.; Tanaka, M. Interactions of traveling fronts: An exact solution of a nonlinear diffusion equation. *Phys. Lett. A* **1983**, *97*, 311–314. [CrossRef]
6. Nucci, M.C.; Clarkson, P. The nonclassical method is more general than the direct method for symmetry reductions. An example of the Fitzhugh-Nagumo equation. *Phys. Lett. A* **1992**, *164*, 49–56. [CrossRef]
7. Li, H.; Guo, Y. New exact solutions to the Fitzhugh–Nagumo equation. *Appl. Math. Comput.* **2006**, *180*, 524–528. [CrossRef]
8. Abbasbandy, S. Soliton solutions for the Fitzhugh–Nagumo equation with the homotopy analysis method. *Appl. Math. Model.* **2008**, *32*, 2706–2714. [CrossRef]
9. Kakiuchi, N.; Tchizawa, K. On an explicit duck solution and delay in the Fitzhugh–Nagumo equation. *J. Differ. Equ.* **1997**, *141*, 327–339. [CrossRef]

10. Schonbek, M.E. Boundary value problems for the FitzHugh-Nagumo equations. *J. Differ. Equ.* **1978**, *30*, 119–147. [CrossRef]
11. Yanagida, E. Stability of travelling front solutions of the FitzHugh-Nagumo equations. *Math. Comput. Model.* **1989**, *12*, 289–301. [CrossRef]
12. Jackson, D. Error estimates for the semidiscrete Galerkin approximations of the FitzHugh-Nagumo equations. *Appl. Math. Comput.*, **1992**, *50*, 93–114. [CrossRef]
13. Gao, W.; Wang, J. Existence of wavefronts and impulses to FitzHugh–Nagumo equations. *Nonlinear Anal. Theory Methods Appl.* **2004**, *57*, 667–676. [CrossRef]
14. Olmos, D.; Shizgal, B.D. Pseudospectral method of solution of the Fitzhugh–Nagumo equation. *Math. Comput. Simul.* **2009**, *79*, 2258–2278. [CrossRef]
15. Dehghan, M.; Heris, J.M.; Saadatmandi, A. Application of semi-analytic methods for the Fitzhugh–Nagumo equation, which models the transmission of nerve impulses. *Math. Methods Appl. Sci.* **2010**, *33*, 1384–1398. [CrossRef]
16. Podlubny, I. *Fractional Differential Equations: An Introduction to Fractional Derivatives, Fractional Differential Equations, to Methods of Their Solution and Some of Their Applications*; Elsevier: Amsterdam, The Netherlands, 1998.
17. Kilbas, A.A.; Srivastava, H.M.; Trujillo, J.J. Theory and applications of fractional differential equations. In *North-Holland Mathematics Studies*; Elsevier Science B.V.: Amsterdam, The Netherlands, 2006; Volume 204, p. 540.
18. Singh, J.; Kumar, D.; Nieto, J.J. A reliable algorithm for a local fractional tricomi equation arising in fractal transonic flow. *Entropy* **2016**, *18*, 206. [CrossRef]
19. Hristov, J. Transient heat diffusion with a non-singular fading memory: From the Cattaneo constitutive equation with Jeffrey's kernel to the Caputo-Fabrizio time-fractional derivative. *Therm. Sci.* **2016**, *20*, 757–762. [CrossRef]
20. Zhao, D.; Singh, J.; Kumar, D.; Rathore, S.; Yang, X.J. An efficient computational technique for local fractional heat conduction equations in fractal media. *J. Nonlinear Sci. Appl. (JNSA)* **2017**, *10*, 1478–1486. [CrossRef]
21. Zaky, M.A.; Machado, J.T. On the formulation and numerical simulation of distributed-order fractional optimal control problems. *Commun. Nonlinear Sci. Numer. Simul.* **2017**, *52*, 177–189. [CrossRef]
22. Ahmadian, A.; Ismail, F.; Salahshour, S.; Baleanu, D.; Ghaemi, F. Uncertain viscoelastic models with fractional order: A new spectral tau method to study the numerical simulations of the solution. *Commun. Nonlinear Sci. Numer. Simul.* **2017**, *53*, 44–64. [CrossRef]
23. Carvalho, A.; Pinto, C.M. A delay fractional order model for the co-infection of malaria and HIV/AIDS. *Int. J. Dyn. Control* **2017**, *5*, 168–186. [CrossRef]
24. Kumar, D.; Singh, J.; Baleanu, D. A fractional model of convective radial fins with temperature-dependent thermal conductivity. *Rom. Rep. Phys*. **2017**, *69*, 103.
25. Patel, H.S.; Patel, T. Applications of Fractional Reduced Differential Transform Method for Solving the Generalized Fractional-order Fitzhugh–Nagumo Equation. *Int. J. Appl. Comput. Math.* **2021**, *7*, 188. [CrossRef]
26. Abdel-Aty, A.-H.; Khater, M.M.; Baleanu, D.; Khalil, E.; Bouslimi, J.; Omri, M. Abundant distinct types of solutions for the nervous biological fractional FitzHugh–Nagumo equation via three different sorts of schemes. *Adv. Differ. Equ.* **2020**, *2020*, 476. [CrossRef]
27. Prakash, A.; Kaur, H. A reliable numerical algorithm for a fractional model of Fitzhugh-Nagumo equation arising in the transmission of nerve impulses. *Nonlinear Eng.* **2019**, *8*, 719–727. [CrossRef]
28. Deniz, S. Optimal perturbation iteration method for solving fractional FitzHugh-Nagumo equation. *Chaos Solitons Fractals* **2021**, *142*, 110417. [CrossRef]
29. Kansa, E.J. Multiquadrics—A scattered data approximation scheme with applications to computational fluid-dynamics-I surface approximations and partial derivative estimates. *Comput. Math. Appl.* **1990**, *19*, 127–145. [CrossRef]
30. Franke, C.; Schaback, R. Convergence order estimates of meshless collocation methods using radial basis functions. *Adv. Comput. Math.* **1998**, *8*, 381–399. [CrossRef]
31. Madych, W.; Nelson, S. Multivariate interpolation and conditionally positive definite functions II. *Math. Comput.* **1990**, *54*, 211–230. [CrossRef]
32. Micchelli, C.A. Interpolation of Scattered Data: Distance Matrices and Conditionally Positive Definite Functions. *Constr. Approx.* **1986**, *2*, 11–22. [CrossRef]
33. Golberg, M.A.; Chen, C.-S.; Karur, S.R. Improved multiquadric approximation for partial differential equations. *Eng. Anal. Bound. Elem.* **1996**, *18*, 9–17. [CrossRef]
34. Sarra, S.A.; Kansa, E.J. Multiquadric radial basis function approximation methods for the numerical solution of partial differential equations. *Adv. Comput. Mech.* **2009**, *2*, 220.
35. Kansa, E.J.; Holoborodko, P. On the ill-conditioned nature of C^∞ RBF strong collocation. *Eng. Anal. Bound. Elem.* **2017**, *78*, 26–30. [CrossRef]
36. Fasshauer, G.E.; McCourt, M.J. *Kernel-Based Approximation Methods Using Matlab*; World Scientific Publishing Company: Singapore, 2015; Volume 19.
37. Uddin, M.; Haq, S. RBFs approximation method for time fractional partial differential equations *Commun. Nonlinear Sci. Numer. Simul.* **2011**, *16*, 4208–4214. [CrossRef]

38. Hussain, M.; Haq, S.; Ghafoor, A. Meshless RBFs method for numerical solutions of two-dimensional high order fractional Sobolev equations. *Comput. Math. Appl.* **2020**, *79*, 802–816. [CrossRef]
39. Rippa, S. An algorithm for selecting a good value for the parameter c in radial basis function interpolation. *Adv. Comput. Math.* **1999**, *11*, 193–210. [CrossRef]